



HAL
open science

Numerical exploration of the impact of hydrological connectivity on rainfed annual crops in Mediterranean hilly landscapes

Mariem Dhouib, Jérôme Molénat, Laurent Prévot, Insaf Mekki, Rim Zitouna-Chebbi, Frédéric Jacob

► To cite this version:

Mariem Dhouib, Jérôme Molénat, Laurent Prévot, Insaf Mekki, Rim Zitouna-Chebbi, et al.. Numerical exploration of the impact of hydrological connectivity on rainfed annual crops in Mediterranean hilly landscapes. *Agronomy for Sustainable Development*, 2024, 44 (6), pp.53. 10.1007/s13593-024-00981-5 . hal-04752688

HAL Id: hal-04752688

<https://hal.science/hal-04752688v1>

Submitted on 24 Oct 2024

HAL is a multi-disciplinary open access archive for the deposit and dissemination of scientific research documents, whether they are published or not. The documents may come from teaching and research institutions in France or abroad, or from public or private research centers.

L'archive ouverte pluridisciplinaire **HAL**, est destinée au dépôt et à la diffusion de documents scientifiques de niveau recherche, publiés ou non, émanant des établissements d'enseignement et de recherche français ou étrangers, des laboratoires publics ou privés.



Distributed under a Creative Commons Attribution 4.0 International License

1 **Numerical exploration of the impact of hydrological connectivity on rainfed annual crops in**
2 **Mediterranean hilly landscapes**

3

4 Mariem Dhouib¹, Jérôme Molénat^{1*}, Laurent Prévot¹, Insaf Mekki², Rim Zitouna-Chebbi², Frédéric
5 Jacob¹

6

7 (1) LISAH, University of Montpellier, AgroParisTech, INRAE, Institut Agros, IRD, 2 place viala,
8 34042 Montpellier Cedex 2, France

9 (2) University of Carthage, National Research Institute of Rural Engineering, Water and Forests,
10 LR16INRGREF02-LRVENC, Rue Hédi Karray, 2080, Ariana, Tunisie

11

12

13 *** Corresponding author** : Jérôme Molénat (orcid : 0000-0002-5957-0927)

14 postal address : LISAH, 2 Place Viala, 34042 Montpellier Cedex, France

15 e-mail address : jerome.molenat@inrae.fr

16

17 Within hilly agricultural landscapes, topography induces lateral transfers of runoff water,
18 so-called interplot hydrological connectivity. Runoff water from upstream plots can infiltrate
19 downstream plots, thus influencing the water content in the root zone that drives crop
20 functioning. The current study aims to comprehensively investigate the impact of runoff on
21 crop functioning in the context of Mediterranean rainfed annual crops. To quantify this
22 impact, we conduct a numerical experiment using the AquaCrop model and consider two
23 hydrologically connected plots. The experiment explores a range of upstream and
24 downstream agro-pedo-climatic conditions: crop type, soil texture and depth, climate forcing,
25 and the area of the upstream plot. The experiment relies on data collected over the last 25
26 years in OMERE, an environment research observatory in northeastern Tunisia, and data
27 from literature. The results show that the downstream infiltration of upstream runoff has a
28 positive impact on crop functioning in a moderate number of situations, ranging from 16%
29 (wheat) to 33% (faba bean) as the average across above ground biomass and yield. Positive
30 impact is mostly found for higher soil available water capacity and under semiarid and dry
31 subhumid climate conditions, with a significant impact of rainfall intra-annual distribution in
32 relation to crop phenology. These results need to be deepened by considering both a wider
33 range of crops and future climate conditions.

34 **Abstract**

35 Within hilly agricultural landscapes, topography induces lateral transfers of runoff water, so-called
36 interplot hydrological connectivity. Runoff water from upstream plots can infiltrate downstream plots,
37 thus influencing the water content in the root zone that drives crop functioning. The impact of runoff
38 on crop functioning can be crucial for optimizing agricultural landscape management strategies.
39 However, to our knowledge, no study has specifically focused on the impact on crop yield. The
40 current study aims to comprehensively investigate the impact of runoff on crop functioning in the
41 context of Mediterranean rainfed annual crops. To quantify this impact, we conduct a numerical
42 experiment using the AquaCrop model and consider two hydrologically connected plots. The
43 experiment explores a range of upstream and downstream agro-pedo-climatic conditions: crop type,
44 soil texture and depth, climate forcing, and the area of the upstream plot. The experiment relies on
45 data collected over the last 25 years in OMERE, an environment research observatory in northeastern
46 Tunisia, and data from literature. A key finding in the results is that water supply through
47 hydrological connectivity can enhance annual crop production, under semiarid and subhumid climate
48 conditions. Specifically, the results show that the downstream infiltration of upstream runoff has a
49 positive impact on crop functioning in a moderate number of situations, ranging from 16% (wheat) to
50 33% (faba bean) as the average across above ground biomass and yield. Positive impact is mostly
51 found for higher soil available water capacity and under semiarid and dry subhumid climate
52 conditions, with a significant impact of rainfall intra-annual distribution in relation to crop phenology.
53 These research needs to be expanded by considering both a wider range of crops and future climate
54 conditions.

55 **Keyword**

56 Hydrological connectivity; Runoff-runon process; Water infiltration; Rainfed agriculture; Annual
57 crops; Crop production; Mediterranean

58

59

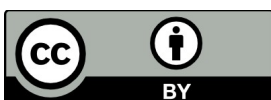


60 1. Introduction

61 Water resources are limited within the Mediterranean basin, with <1,000 m³/capita/yr in the eastern
62 and southern Mediterranean (Fader et al. 2020). These resources are unevenly distributed in time and
63 space, partly due to contrasting rainfall patterns (Blinda and Thivet 2009; Daccache et al. 2016; Fader
64 et al. 2020). This water context is set to worsen because of (1) water resource over-exploitation to
65 meet the growing food demand (Karabulut et al. 2018; Souissi et al. 2019) and (2) climate change
66 consequences such as rainfall decreases, up to 30% (Lange et al. 2020), an increase of evaporative
67 demand (Fader et al. 2020) and a concentrations of intra-annual rainfall distributions (Ramos and
68 Martínez-Casasnovas 2006). As the largest water user, the agricultural sector has long been under
69 threat, with subsequent challenges for food security (Yang and Zehnder 2002). Rainfed annual crops
70 are significantly affected by water issues because (1) they fully depend upon rainfall as a water
71 resource, and (2) their shallow root systems make them vulnerable to water shortages (Hossain et al.
72 2020).

73 Mediterranean policies for water resources management have mainly oriented to support irrigated
74 agriculture (Besbes et al. 2014; Nouri et al. 2020). As a result, less attention has been given to rainfed
75 agriculture, which uses less water per unit area (Anderson et al. 2016). Nevertheless, it would be
76 possible to further improve rainfed agricultural productivity by implementing strategies that
77 (1) reduce crop water needs, with species suited to drought conditions, or (2) increase water
78 availability in the root zone by favoring runoff/rainwater infiltration or minimizing evaporative losses.
79 The amount of water that infiltrates the root zone can be increased using water harvesting techniques
80 (e.g., planting pits, terraces) at different spatial scales, from plot to landscape (Yadari et al. 2019;
81 Tadros et al. 2021; Molénat et al. 2023). These techniques are suitable for landscapes with hilly
82 topography that allows for the spatial redistribution of surface runoff (Ammar et al. 2016; Mekki et al.
83 2018). The benefits of these techniques in reducing runoff, promoting infiltration, increasing the soil
84 water content, and enhancing crop yield have been demonstrated, particularly in Sub-Saharan Africa
85 (see Wolka et al. (2018) for a review). Most of the studies conducted in the Mediterranean basin have
86 demonstrated the benefits of the techniques in terms of reducing runoff or increasing the soil water
87 content (Schiettecatte et al., 2005). To our knowledge, no study has specifically focused on the impact
88 on crop yield.

89 Hydrological connectivity refers to water transfer across different areas of the landscape (Bracken
90 and Croke, 2007). In Mediterranean hilly landscapes, surface runoff predominantly drives interplot
91 hydrological connectivity, redistributing rainfall between plots. This runoff-runon process occurs
92 when runoff from upstream plots infiltrates downslope cultivated plots with greater infiltration
93 capacity (Jones et al., 2013; Van Loo and Verstraeten, 2021), thus enhancing water availability in the
94 root zone (Fig. 1)(Howes and Abrahams, 2003). While the impact of interplot hydrological



95 connectivity on hydrological processes like stream flow generation is well recognized (Nanda et al.,
96 2019; Zuecco et al., 2019; Saco et al., 2020), few studies evaluate its effect on crop functioning.
97 Typically, crop functioning is studied using multilocal methods that assume hydrological
98 independence among plots, overlooking the influence of hydrological connectivity (Van Gaelen et al.,
99 2017). However, understanding this impact is crucial for optimizing agricultural landscape
100 management strategies, particularly in arid to semiarid Mediterranean regions where water scarcity is
101 a primary limiting factor for crop growth (Daccache et al., 2016; Araya et al., 2017) and where lateral
102 water transfer primarily occurs through surface runoff (Mekki et al., 2006).

103 Studying the impact of interplot hydrological connectivity on rainfed annual crops in hilly
104 Mediterranean regions requires careful consideration of key environmental factors affecting both
105 downstream crop functioning and upstream runoff generation. Considering these factors enables the
106 exploration of their potential influence on hydrological connectivity. Various elements can influence
107 surface runoff, including rainfall patterns (Chen et al. 2016), hydrodynamic properties, soil moisture
108 (Schoener and Stone 2019), agricultural practices (Prosdocimi et al. 2016), vegetation cover type
109 (Nunes et al. 2011; Liu and Lobb 2021), and the impluvium area, representing the upstream
110 contributing area for runoff input (Gnouma 2006). Furthermore, the functioning of downstream crops
111 can be affected by the infiltration of upstream runoff and other environmental factors, such as climate
112 (comprising rainfall and evapotranspiration demand), soil properties (such as the organic matter
113 content and available water capacity), and agricultural practices (including fertilization and soil
114 management) (Mbava et al. 2020). Investigating the potential influences of these environmental
115 factors on hydrological connectivity can be pursued through field campaigns or numerical
116 experiments using modeling. The latter approach is more suitable, as it allows for (1) the
117 consideration of a wide range of environmental factors and (2) the disentanglement of the combined
118 effects of environmental factors with hydrological connectivity.

119 The objective of this article is to study the impact of water infiltration due to the runoff-runon
120 process on crop functioning. We focus on rainfed annual crops in a Mediterranean hilly landscape,
121 emphasizing two main agronomic variables: above ground biomass and yield. In Section 2, we
122 introduce the numerical experiment by describing the chosen modeling approach, the various
123 influential factors to consider, and the strategy for analyzing the results. Section 3 presents and
124 discusses the analysis of modeling simulations: we first examine the occurrence of situations with a
125 significant impact on hydrological connectivity and then assess the importance of environmental
126 conditions (climate, upstream runoff, soil texture and depth) on this impact. Finally, we discuss the
127 prospects of this study, considering that it represents a preliminary step toward an integrated
128 catchment-scale approach.

129

[Fig. 1 about here.]



130

131 2. Materials and methods

132 2.1. General framework

133 The numerical experiment is based on simulating crop functioning in a downstream plot receiving
134 surface runoff from an upstream plot that is hydrologically connected, and by considering crops, soils
135 and climate typical of Mediterranean conditions (Fig. 2). The downstream plot is supplied with water
136 from both rainfall and runoff simulated in the upstream plot. Assumptions include homogeneity in
137 parameters, state variables, and fluxes within each plot, as well as complete transfer of upstream
138 runoff to the downstream plot due to hydrological connectivity. Here, we provide an overview of the
139 numerical experiment setting, and a detailed presentation is provided in Supplementary materials -
140 Section 1.

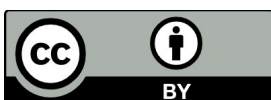
141 The numerical experiment is conducted using the AquaCrop model (Raes et al. ,2009; Steduto et
142 al., 2009), chosen for its performances to simulate crop functioning as well as surface runoff in water-
143 driven conditions typical of arid to semiarid Mediterranean regions. Furthermore, AquaCrop has been
144 extensively validated for a range of state variables related to water budgets and crop growth across
145 various Mediterranean conditions (Garcia-Lopez et al, 2014, Toumi et al., 2016), especially under the
146 conditions considered in the current study (Dhouib et al., 2022).

147 [Fig. 2 about here.]

148 The simulations of downstream crop functioning with additional water supply from upstream
149 runoff, span a wide range of typical Mediterranean conditions. This includes a diversity of
150 environmental drivers that influence crop functioning, such as (1) varying crop types with distinct
151 hydrological functioning and phenology , (2) different soil available water capacity in relation to
152 varying soil depth and texture via hydrodynamic properties (Cousin et al. 2022), and (3) inter- and
153 intra-annual variability of climate forcing over decades, including rainfall, temperature and reference
154 evapotranspiration.

155 In the downstream plot, we consider a range of upstream runoff magnitudes to account for the
156 Mediterranean hydrological variability. The upstream runoff is simulated based on environmental
157 factors like crop type, soil available water capacity, and climate forcing. An additional factor is the
158 drained area of the upstream plot , hereafter referred to as the impluvium, characterized using the ratio
159 of upstream to downstream plot areas. A low ratio indicates a downstream plot near a hillslope
160 summit in a landscape, while a high ratio signifies a downstream plot along or at the bottom of a
161 hillslope.

162 To simulate typical Mediterranean conditions, we use the OMERE observatory database



163 (www.obs-omere.org, Molénat et al. 2018), that meets specific requirements. It encompasses a range
164 of climate forcings that spans the last three decades and observations collected within the Kamech
165 catchment (Cap Bon Peninsula, northeastern Tunisia) that is representative of semiarid Mediterranean
166 regions in terms of crops, soil, and climate.

167 2.2. Overview of the AquaCrop crop model

168 Detailed presentations of AquaCrop (<https://www.fao.org/aquacrop/en/>) are provided by Raes et al.
169 (2009) and Steduto et al. (2009). Here, we outline the specificities related to our methodological
170 choices.

171 AquaCrop is a crop model designed to simulate crop functioning and the principal components of
172 the water balance. Specifically, tailored for arid and semiarid environments, it is categorized as a
173 water-driven model (Todorovic et al. 2009). Indeed, it adjusts crop growth based on vegetation
174 transpiration, itself driven by root zone soil moisture. This characteristic makes it well suited for
175 Mediterranean regions, where water acts as the principal limiting factor for agricultural production.

176 AquaCrop simulates, on a daily time step, the components of soil water balance across the soil–
177 plant-atmosphere continuum (infiltration and runoff, deep percolation and capillary rise, soil
178 evaporation and vegetation transpiration), as well as plant growth and production (canopy crop cover,
179 root growth, above ground biomass, yield). Crop transpiration (Tr) is derived from canopy crop cover
180 (CC) and reference evapotranspiration (ET_0). Above ground biomass (AGB) is then derived from Tr
181 and normalized water productivity (WP^*), which accounts for atmospheric CO_2 concentration. Yield
182 (Yld) is calculated as the product of AGB and the harvest index (HI). Runoff is determined using the
183 empirical curve number method that accounts for crop type, agricultural practice, and hydrological
184 soil group in relation to the soil infiltration rate and antecedent soil moisture. The soil water balance is
185 calculated by discretizing the soil into five horizons based on pedological characteristics.

186 The AquaCrop forcing variables encompass climate data (e.g., air temperature, reference
187 evapotranspiration ET_0 , rainfall, and atmospheric CO_2 concentration) on a daily timescale. The model
188 parameters consist of soil properties (texture and depth, soil moisture at field capacity, permanent
189 wilting point and saturation, saturated hydraulic conductivity), cultural parameters (e.g., maximum
190 canopy cover, crop coefficient), and agricultural practice data (e.g. fertilization, sowing date).

191 2.3. Setting the agro-pedo-climatic conditions

192 We assumed the same variability for the agro-pedological conditions within the upstream and
193 downstream plots. All possible scenarios for each of the two plots are next combined to ensure the
194 representativeness of the resulting AquaCrop simulations. When dealing with climate conditions,
195 including rainfall, air temperature and ET_0 , for instance, we assumed uniformity across the two plots.



196 2.3.1. Crop types and subsequent crop parameters

197 We chose wheat as the cereal crop and faba bean as the legume crop for two main reasons. First, they
198 are among the main rainfed crops in the Kamech catchment (Mekki et al. 2006) and the broader
199 Mediterranean region (Jourdan, 2022). Second, wheat and faba bean differ significantly in
200 phenological cycle duration, agricultural practices (sowing and harvest dates) and in hydrological
201 functioning (different soil cover rates implying different infiltration-runoff ratios). Faba bean, a row
202 crop with a short phenological cycle, contrast with wheat, a cover crop with a longer phenological
203 cycle. Crop parameters for wheat and faba bean used in the model are detailed in the Table 1.
204 Supplementary materials - Sections 2 details the setting, according to the study area, of the choice of
205 sowing dates and the fertilization rates.

206 [\[Table 1 about here.\]](#)

207 2.3.2. Soil characteristics and hydrodynamic properties

208 Soil hydrodynamic properties include (1) soil moisture at field capacity (FC), at permanent wilting
209 point (PWP), and at saturation (Sat), as well as (2) the saturated hydraulic conductivity (Ksat). These
210 properties are determined based on soil textures estimated from 10 soil pits collected at various
211 locations within Kamech catchment according to the USDA classification (Coulouma et al. 2017).
212 Then, the soil textures are converted into hydrodynamic properties using the nominal values proposed
213 by the AquaCrop user guide (Table 2). Three different depths, namely, 0.5 m, 1 m, and 1.5 m are
214 chosen on the basis of the variability of soil depth observed in Kamech catchment (Molénat et al.
215 2018). By combining three soil textures and three soil depths, we simulate nine situations for soil
216 available water capacity.

217 [\[Table 2 about here.\]](#)

218 2.3.3. Climate forcing

219 A 25-year climate period from September 1, 1995, to August 31, 2019 is chosen, corresponding to the
220 maximum window for which the OMERE data are available. The climate forcing data are air
221 temperature, rainfall, reference evapotranspiration ET_0 .

222 For this climate series, the annual averages for rainfall, air temperature during the vegetation
223 growing season (October to May) and ET_0 are 629 mm, 14.8°C and 1310 mm, respectively
224 (Supplementary Materials - Section 3, Fig. SF2). The years 1996 and 2019 are the wettest, with
225 cumulative rainfall of 1036 mm and 862 mm, respectively. The years 1997, 2002 and 2016 are the
226 driest, with cumulative rainfall of 406 mm, 394 mm and 416 mm, respectively. Regarding air
227 temperature, 1999 and 2009 are the coldest years, with an average air temperature of 14.2°C over the
228 crop growth period [October - May]. The years 2001, 2002 and 2007 are the warmest, with an average



229 air temperature of 15.4°C over the crop growth period [October - May] (Supplementary Materials -
230 Section 3, Fig. SF2).

231 To deepen the analysis of AquaCrop simulations, we classify the years of the climate series using
232 the FAO aridity index (Spinoni et al. 2014). This index expresses aridity as the ratio of atmospheric
233 water supply (rainfall) to atmospheric water demand (ET_0). We opt for this index because (1) it
234 considers several climate variables when using ET_0 to quantify aridity, and (2) it is suitable for
235 analyzing AquaCrop simulations since AquaCrop involves ET_0 when calculating the above ground
236 biomass. According to the FAO aridity index, the climate series comprises two subhumid years (SH),
237 10 dry subhumid years (DSH), and 13 semiarid years (SA), accounting for occurrences of 8%, 40%,
238 and 52%, respectively (Fig. 3). Additional details about the calculation of the FAO aridity index are
239 provided in the Supplementary Materials - Section 3.

240 [Fig. 3 about here.]

241 **2.4. Simulating the upstream runoff**

242 The upstream runoff is quantified using AquaCrop simulations based on the agro-pedo-climatic
243 conditions discussed in Section 2.3. The agro-pedo-climatic conditions include two crop types, nine
244 situations for soil available water capacity (three soil textures and three soil depths), and 25 years of
245 climate. To account for the impluvium area, simulated upstream runoff is weighted by the α ratio, that
246 is, the ratio of the upstream to the downstream plot area (Fig. 2), which is set to three nominal values:
247 0.5, 1 and 2. By combining two crop types, nine conditions for soil available water capacity, and three
248 ratios of the upstream to the downstream plot area, we obtain 54 situations of upstream runoff and
249 thus 54 simulated time series of runoff, each spanning 25 years. Subsequently, each simulated time
250 series of upstream runoff is added to the corresponding time series of rainfall in the downstream plot.

251 The set of simulated time series of upstream runoff, after weighting by the α ratio, depicts a range
252 of annual cumulative values from 9 mm to 691 mm, representing 2% to 97% of the annual rainfall,
253 depending on the year. To further analyze the impact of upstream runoff on downstream crop
254 functioning, we classify these annual cumulative values into four classes relative to three quartiles
255 (Table 3). We refer hereafter to classes of upstream runoff.

256 [Table 3 about here.]

257 **2.5. Simulating downstream crop functioning**

258 Downstream crop functioning is simulated with AquaCrop, considering the agro-pedo-climatic
259 conditions (Section 2.3) and the upstream runoff (Section 2.4). For each of the two downstream crops
260 (wheat and faba bean) and each of the nine downstream situations in terms of soil available water
261 capacity, 54 AquaCrop simulations are run, varying in the simulated input of upstream runoff. This

262 results in 486 simulations for each of the two downstream crops to be linked for comparison purposes
263 to the corresponding nine reference simulations (3 soil depths, 3 soil textures) of crop functioning
264 without upstream runoff from connectivity. On a yearly basis, these 486 simulations amount to 12,150
265 simulations for each downstream crop, totaling 24,300 for both.

266 2.6. Simulation analysis

267 To study the impact of water infiltration due to the runoff-runon process on downstream crop
268 functioning, we focus on two agronomic variables driven by crop functioning, namely, above ground
269 biomass (AGB) and yield (Yld). We conduct a quantitative analysis, which involves calculating the
270 relative differences in AGB and Yld between simulations with and without connectivity (Equation 1,
271 X_{wc} and X_{oc} stand for the value of the simulated variable with and without connectivity,
272 respectively). This allows us to (1) globally quantify, for all considered situations, the impact of
273 upstream runoff by hydrological connectivity on the functioning of the downstream crops (wheat and
274 faba bean) and (2) understand the influence, on this impact, of environmental conditions within the
275 downstream plot (upstream runoff, climate forcing, soil texture and depth, crop).

$$276 \quad \Delta (AGB \text{ or } Yld) = \frac{X_{wc} - X_{oc}}{X_{oc}} \quad (\text{Equation 1})$$

277

278 For each of the two downstream crops, the relative difference Δ is calculated at the annual timescale
279 along the 25-year time series for any of the 486 combinations (3 soil depths, 3 soil textures, 54
280 upstream runoff). A year Y is considered a hydrological year spanning from the beginning of
281 September of the calendar year $[Y-1]$ to the end of August of the calendar year $[Y]$. This results in a
282 total of 12,150 relative differences calculated for AGB and Yld for each crop in the downstream plot
283 and for each of the 25 years. $\Delta > 0$ (< 0) indicates that additional water input through hydrological
284 connectivity has a positive (negative) impact, since it leads to an increase (a decrease) in AGB and
285 Yld compared to the case without connectivity.

286 Before analyzing all relative differences Δ , it is necessary to define criteria for selecting only
287 realistic and accurate simulations used in the analysis :

288 ● The first criteria relies on the crop yield. For this, we filter AquaCrop simulations based on an
289 agro-economic constraint, namely, yield. Following field-based expert recommendations, we
290 select simulations with Yld (wheat) > 0.5 ton/ha and Yld (faba bean) > 0.25 ton/ha, knowing that
291 yields below these values are considered null from an agro-economic constraint. To avoid
292 eliminating significant impact changes between with and without connectivity, this filter is applied
293 to simulations with connectivity if $\Delta > 0$ and without connectivity if $\Delta < 0$.

294 ● A second criteria defines a threshold value for a significant change (Δ) to account for uncertainties
295 in the AquaCrop simulations. For this, we refer to Dhouib et al. (2022), who reported that the



296 model satisfactorily simulates AGB, with a relative error between observations and simulations of
297 approximately 11%. Therefore, we choose a threshold of 0.11 for the absolute value for Δ , above
298 which the impact of water input through connectivity is considered significant as it exceeds the
299 modeling uncertainty. If negative (positive) Δ values are greater (lower) than or equal to -0.11
300 (0.11), we consider that the impact of water input through hydrological connectivity on crop
301 functioning is insignificant. Since the model has not been evaluated for yield in the study area, we
302 use the same threshold on Δ for AGB and Yld.

303

304 3. Results and discussion

305 3.1. Above ground biomass (AGB) and yield (Yld)

306 The analysis of relative differences between simulations with and without connectivity indicates that
307 in most situations (combinations of soil available water capacity derived from soil texture and depth,
308 upstream runoff, and climate year), the contribution of hydrological connectivity through runoff
309 infiltration has a nonsignificant impact on AGB/Yld. This holds true for both downstream crops of
310 wheat and faba bean, with more than 85%/77% and 67%/62% of the calculated differences falling
311 between -0.11 and 0.11, respectively (Fig. 4, Fig. SF3 and SF4 un Supplementary Materials – Section
312 4).

313

[Fig. 4 about here.]

314 Beyond the overall results, there are situations in which the contribution of hydrological
315 connectivity through runoff infiltration significantly increases AGB and Yld for both wheat and faba
316 bean crops. The increase is more pronounced for faba bean than for wheat, with 33% of the relative
317 differences (average over AGB and Yld values) being greater than 0.11 for faba bean, compared to
318 16% only for wheat. This suggests that faba bean is more sensitive to water shortages than wheat and
319 that additional water input via the infiltration of upstream runoff contributes to alleviating this
320 shortage. This is confirmed by the analysis of the water stress coefficient K_s . Indeed, in 69% of the
321 situations considered, faba bean is more often stressed than wheat since it has a lower K_s (Fig. SF5 in
322 Supplementary Materials - Section 5), while the increase in K_s induced by upstream runoff averages
323 9% for faba bean and only 2% for wheat (data not shown). This greater sensitivity of faba bean to
324 water shortage can be explained by (1) a shorter phenological cycle, making its functioning more
325 sensitive to intra-annual variations in rainfall, and (2) a shorter root system (Hamblin and Tennant
326 1987) that does not allow the crop to use water stored in deeper soil layers. These simulation results
327 converge with the observations of Daryanto et al. (2017), who reported a drought-based yield
328 reduction more important for legume crops than for cereal crops.

329 When a positive impact is observed, the increase induced by water input through hydrological

330 connectivity is higher for grain yield (Yld) than for above ground biomass (AGB). This is ascribed to
331 the way that AquaCrop calculates Yld as the product of AGB and the harvest index (HI), where HI is
332 sensitive to water stress (Ali and Talukder 2008; AquaCrop user manual). Thus, the latter has a
333 double effect on Yld via both AGB and HI.

334 We also observe another type of situation, much rarer (only 3% of relative differences), where
335 water input through hydrological connectivity leads to negative relative differences (Fig. 4). This
336 indicates a decrease in both above ground biomass (AGB) and yield (Yld), which may be attributed to
337 waterlogging (Liu et al. 2020). Since the frequency of such a situation is low, we mainly focus on
338 situations with a positive impact of hydrological connectivity for the remainder of this paper.

339 3.2. Influence of environmental conditions

340 We investigate the influence of environmental conditions of the downstream plot (hydrological
341 conditions, soil texture and depth, and climate) to understand how some of these conditions can lead
342 to positive impacts. For each downstream crop, we categorize the set of significant Δ values
343 ($\Delta > 0.11$) for both above ground biomass (AGB) and yield (Yld) based on the respective classes of a
344 given environmental factor (i.e., four classes for upstream runoff, three classes for texture, three
345 classes for soil depth and three classes for climate years). Thus, the cumulative distribution across all
346 classes for any environmental factor and any Δ type (AGB, Yld) adds up to 100%. The resulting
347 statistics are presented in Tables 4, ST3, ST4 and ST6 and are utilized in the subsequent three
348 subsections.

349 [\[Table 4 about here.\]](#)

350 3.2.1. Hydrological conditions

351 We emphasize three significant results related to the simulated water dynamics, from runoff to the soil
352 water content, in connection with AGB and Yld variations.

353 First, in situations with insignificant impact ($\Delta \in [-0.11 ; +0.11]$), the occurrences of the Δ values are
354 evenly distributed across the four classes of upstream runoff (Supplementary materials - Section 6,
355 Table ST3). In situations with positive impact, the occurrences of the Δ values are lower for the first
356 two classes of upstream runoff that correspond to the lowest cumulative values (R1 and R2 classes in
357 Table 3), as they account for 40% to 46% of cases depending on the crop and the production variable
358 (AGB or Yld). Conversely, the occurrence of the Δ values is larger for the last two classes (R3 and
359 R4) that correspond to the highest cumulative values, with 54% to 60% of cases.

360 Second, in situations with a positive impact, the increase in the water infiltration amount induced by
361 upstream runoff averages 10% and 7% relative to wheat and faba bean, respectively (Table ST4).
362 Meanwhile, the increase in infiltration for situations with an insignificant impact is only 8% and 6%
363 for the two crops.



364 Third, situations with a positive impact show an average increase in the simulated root zone water
365 content (wRZ) over the crop cycle of 41% and 24% for wheat and faba bean, respectively (Table
366 ST4). In contrast, for situations with an insignificant impact, the simulated root zone water content
367 increases by only 2% and 1% for these crops.

368 From these three main results, we can infer first and clearly that the hydrological connectivity in
369 Mediterranean regions can have an impact on crop growth. Nevertheless, these results suggest that the
370 increase in AGB and Yld depends only partially on the amount of upstream runoff. While positive
371 impact situations are predominantly associated with a significant increase in upstream runoff, even
372 small increases in upstream runoff (Class R1 in Tables 3 and ST3) and in the resulting infiltration
373 (Table ST3) can also lead to positive impacts. For our case study, the impact of hydrological
374 connectivity through the runoff-runon process on crop production seems to be primarily determined
375 by the increase in the root zone water content during the crop cycle. Our study suggests thus that the
376 impact of hydrological connectivity is not solely determined by the total annual water amount brought
377 by runoff and subsequent infiltration to downslope plot. Rather it is more influenced by the
378 relationship between runoff (and subsequent infiltration) and the increase of soil water in the root
379 zone during the crop cycle. The remaining results of our study provide insights in this relationship.

380

381 3.2.2. Soil texture and depth

382 For both crops (wheat and faba bean) and both agronomic variables (above ground biomass AGB and
383 yield Yld), the deeper the soil, the larger the occurrence of significant Δ values (Table 4). Indeed, the
384 occurrence intervals are [12% - 15%], [31% - 42%], and [43% - 57%] for 0.5, 1, and 1.5 m deep soil,
385 respectively. When dealing with soil texture, a large occurrence of significant Δ values is observed for
386 clay-loam (CL) soils, with an average value of 47% when merging the two crops and two agronomic
387 variables (Table 4). Compared to CL soils, lower occurrences are observed for C and SCL, with
388 average values (over the two crops and two agronomic variables) of 30% and 24%, respectively
389 (Table 4).

390 These results are consistent with the concept of soil available water capacity and align with recent
391 literature on this topic. We observed increases in above ground biomass (AGB) and yield (Yld)
392 following the infiltration of upstream runoff, mainly for clay-loam (CL) soils and deeper soils. This
393 observation is explained by (1) a larger soil available water capacity for CL and deeper soils, allowing
394 for a greater storage of water in the root zone (Alkassem et al. 2022; Cousin et al. 2022) and (2) a soil
395 conducive to root zone development in terms of depth (van Leeuwen 2022).

396 To illustrate these statements, we use the example of wheat sown in 2002 in clay-loam soil and
397 compare crop functioning across the three soil depths considered (Fig. 5). For the same temporal
398 pattern and amount of water received from upstream runoff through hydrological connectivity (α ratio



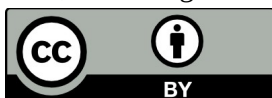
399 is 2 in the simulations of Fig. 5), the above ground biomass increases from 1.5 ton/ha at a soil depth
400 of 0.5 m to 6.1 ton/ha at a soil depth of 1.5 m. This difference can be explained by changes in the root
401 zone water content in relation to soil depth. Indeed, upstream runoff increases the amount of water
402 that infiltrates into the soil by 8% for the three soils between simulations with and without
403 connectivity (data not shown). This further increases wRZ by 2%, 35% and 88% for the 0.5 m, 1 m
404 and 1.5 m soil depths, respectively, between simulations with and without connectivity (data not
405 shown). These changes in the root zone water content can be related to changes in crop functioning
406 throughout the crop growth cycle, as discussed below.

- 407 ● The comparison of crop functioning variables for different soil depths, including water storage in
408 the root zone, transpiration, canopy cover, and above ground biomass, suggests that from the
409 beginning of the crop cycle to January 10, the wheat crop exhibits a similar rooting depth for the
410 three soil depths, thus accessing the same amount of water in the soil.
- 411 ● From January 10 onwards, the crop roots continue to expand downward in the 1 m and 1.5 m deep
412 soils, while they reach their maximum growth in the shallow soil (0.5 m depth). Consequently, the
413 root zone water content decreases for the crop in the shallow soil (0.5 m depth), whereas it
414 increases for the crop in the deeper soils (1 m and 1.5 m depth). This leads, for the shallow soil, to
415 reductions in canopy cover (CC), crop transpiration (Tr), and above ground biomass (AGB)
416 50 days later (March 1) when the root zone water content reaches a critical level. Conversely, these
417 reductions are not observed for the crop in the 1 m and 1.5 m deep soils that still benefit from
418 sufficient water content within the root zone.
- 419 ● For wheat sown in 1 m and 1.5 m deep soils, the initial deviation between the two temporal courses
420 of the root zone water content occurs on March 2. Specifically, the root zone water content slightly
421 increases for the 1.5 m deep soil due to deepening root growth, whereas it decreases for the 1 m
422 deep soil as the root system has reached its maximum depth. This leads, for the 1 m depth soil, to
423 reductions in CC, Tr, and AGB 50 days later (April 15), when the soil water content reaches a
424 critical level. Conversely, these reductions are not observed until senescence of the crop in the
425 1.5 m deep soils that still benefit from sufficient water content within the root zone.

426 [Fig. 5 about here.]

427 3.2.3. Climate forcing

428 When the influence of climate conditions is analyzed, the increases in above ground biomass (AGB)
429 and yield (Yld) due to water input through hydrological connectivity are primarily noticeable in dry
430 subhumid (DSH) and semiarid (SA) years, while being almost negligible in subhumid (SH) years
431 (Table 4). Indeed, occurrence intervals for significant Δ values ($\Delta > 0.11$) are [0% - 5%],
432 [40% - 49%], and [46 - 60%] for the SH, DSH, and SA years, respectively. For wheat, 0% of
433 significant Δ values are observed in SH years, 42% in DSH years, and 58% in SA years. For faba
434 bean, 4% of significant Δ values are observed in SH years, and the remainder are evenly distributed



435 between DSH and SA years (approximately 48%). Notably, these results may be biased by the
436 uneven distribution of climate years, comprising 8% of SH years, 40% of DSH years, and 52% SA
437 years. This uneven distribution is an inherent limitation of the study that relies on field observations
438 of climate forcing, although the distribution of significant Δ values does not completely align on that
439 of climate years.

440 **3.2.3.1. During semi-arid years**

441 During SA years, the downstream infiltration of upstream runoff, even in small quantities,
442 increases the water content in the root zone, thereby increasing AGB and Yld. On average, during
443 these years, the increase in the soil water content in the root zone due to upstream runoff is 29% for
444 wheat and 18% for faba bean (Supplementary materials - Section 6, Table ST5). The example of the
445 year 2016 is characteristic of the increase in the root zone water content induced by infiltration. This
446 year is classified as an SA year according to the FAO aridity index (Fig. 3), with annual rainfall
447 accumulation largely below the 25-year average (Supplementary materials - Section 3, Fig. SF2).
448 During this year, the downstream plot benefits from additional runoff between a lower value of 9 mm
449 and an upper value of 105 mm (data not shown), depending on the environmental conditions of the
450 upstream plot (soil, crop, and impluvium area). For the two limits mentioned above, infiltration in the
451 downstream plot (cultivated with wheat) increases by 1% and 18%, respectively, wRZ increases by
452 4% and 29%, AGB increases by 27% and 112%, and Yld increases by 35% and 406% (median values
453 of all downstream soils, data not shown).

454 **3.2.3.2. During dry subhumid years**

455 The influence of climate forcing on the increase in above ground biomass (AGB) and yield (Yld)
456 may be linked to the intra-annual variability in rainfall, especially in dry subhumid years. Indeed,
457 when analyzing the occurrences of positive impact, calculated for faba bean in dry subhumid years
458 considering all downstream soil textures and depths and all runoff amounts (Supplementary
459 Materials - Section 7, Fig. SF6), we note the following trends.

- 460 ● On the one hand, water input through hydrological connectivity has a frequent positive impact on
461 AGB and Yld (occurrence > 10% in Fig. SF6) for a group of years, namely, 1998, 1999, 2004,
462 2010, and 2013. These years are characterized by annual rainfall accumulations of 750 mm,
463 700 mm, 708 mm, 650 mm, and 622 mm, respectively (Supplementary materials - Section 3,
464 Fig. SF2).
- 465 ● On the other hand, water input through connectivity has a less frequent positive impact on AGB
466 and Yld (occurrence < 10% in Fig. SF6) for 2003, 2005, and 2009, characterized by very similar
467 annual rainfall accumulations: 728 mm, 651 mm, and 793 mm, respectively Supplementary
468 materials - Section 3, Fig. SF2).

469 Therefore, the infiltration of runoff water from upstream is more likely to increase the above ground



470 biomass (AGB) and yield (Yld) of the faba bean crop for the first group of years, but this is less likely
471 for the second group. To gain further insight into this observation, we examine simulations without
472 hydrological connectivity considering a clay-loam soil with a 1 m depth for two dry subhumid years:
473 in 2003 (728 mm of rainfall), the occurrence of positive impacts among all tested situations is rather
474 low (8%), whereas it is much greater (61%) in 2004 (708 mm of rainfall) (Supplementary Materials -
475 Section 7, Fig. SF6). In the situation without hydrological connectivity, AGB and Yld are lower in
476 2004 than in 2003. Therefore, the potential crop production increase by upstream runoff is higher for
477 2004 than for 2003. The analysis of monthly rainfall (Fig. 6a) reveals differences in the intra-annual
478 distribution of rainfall between the two years, leading to subsequent variations in crop growth.

479 ● During the hydrological year 2004, September, December, and March are characterized by high
480 monthly rainfall, thereby increasing the amount of water that infiltrates into the soil (Fig. 6c). In
481 contrast, the hydrological year 2003 has a drier start compared to 2004 (except for November).
482 From January onwards, the rainfall in 2003 is more substantial than that in 2004. This intra-annual
483 distribution of rainfall results in a higher water content in the root zone between September and
484 February in 2004 than in 2003 (Fig. 6d). However, this difference in the soil water content
485 between the two years does not have a particularly positive impact on the growth of faba bean in
486 2004, as the crop is in the early stages of its cycle (Fig. 6e).

487 ● From February onwards, the water content in the root zone in 2003 is higher than that in 2004 due
488 to greater rainfall in January, February, and April. This explains the better vegetation development
489 in 2003.

490 [Fig. 6 about here.]

491 To compare the impact of hydrological connectivity on crop production during these two years (2003
492 and 2004), we consider the same agro-pedological situation considered above (faba bean cultivated in
493 a clay-loam soil with 1 m depth) for a downstream plot receiving typical upstream runoff (from an
494 upstream plot cultivated with faba bean in a 1 m deep clayey soil). Then, water input from
495 hydrological connectivity increases infiltration and wRZ by 8% and 10%, respectively, in 2004 and
496 by 11% and 6% in 2003, respectively. Furthermore, the resulting increase in yield is far larger in 2004
497 (73%) than in 2003 (13%), which is ascribed to the intra-annual variability in rainfall discussed above.

498

499 **4. Conclusion**

500 We report the first complete numerical experiment aimed at quantifying the impact of hydrological
501 connectivity between plots on Mediterranean rainfed crop production.

502 The results show that water input through hydrological connectivity has a positive impact on
503 agricultural production depending on environmental conditions related to crops, climate forcing, and



504 soil properties. Climate forcing significantly influences the impact of hydrological connectivity from
505 both yearly rainfall and the intra-annual distribution of rainfall. A positive impact is observed in dry
506 subhumid and semiarid climate years, suggesting that this impact may become more pronounced in
507 light of the forecasted climate change.

508

509 These novel results pave the way of optimizing agricultural landscape management strategies.
510 Future investigation should expand environmental conditions and address the current study's
511 assumptions. It should include detailed spatial and temporal variability in agricultural plots,
512 considering how upstream runoff and agricultural practices modify soil properties. The cumulative
513 impact of runoff across successive plots and the role of subsurface water flow, particularly in hilly
514 Mediterranean regions, also need investigation. Lastly, coupling crop models with distributed
515 hydrological models could enhance the relevance of runoff simulations within cultivated landscapes.

516

517

518 **Acknowledgements**

519 The OMERE observatory (www.obs-omere.org), funded by the French institutes INRAE and IRD and
520 coordinated by INAT Tunis, INRGREF Tunis, UMR Hydrosociences Montpellier and UMR LISAH
521 Montpellier, is acknowledged for providing a portion of the data used in this study. The OMERE
522 observatory is part of OZCAR Research Infrastructure (<https://www.ozcar-ri.org/>) that is supported
523 by the French Ministry of Research, French Research Institutions and Universities.

524 **Funding**

525 This work was financially supported by the Tunisian Ministry of Higher Education and Scientific
526 Research (MESRS), the French National Research Institute for Sustainable Development (IRD). The
527 current study is part of the ALTOS project in the framework of the PRIMA 2018 program, with
528 financial contributions from France and Tunisia. A CC-BY public copyright license has been applied
529 by the authors to the present document and will be applied to all subsequent versions up to the Author
530 Accepted Manuscript arising from this submission, in accordance with the grant's open access
531 conditions.

532 **Conflicts of interest/Competing interests**

533 The authors have no conflicts of interest to declare that are relevant to the content of this article.

534 **Ethics approval**

535 Not applicable.

536 **Consent to participate**

537 Not applicable

538 **Consent for publication**

539 Not applicable

540 **Availability of data and material**

541 The datasets generated during and/or analysed during the current study are available from the
542 corresponding author on reasonable request.

543 **Code availability**

544 Code will be made available on request

545

546 **Authors' contributions**



547 Conceptualization, F.J., I.M., J.M., L.P. and R.Z-C.; Methodology, F.J., J.M., L.P. and M.D.;
548 Software, M.D.; Validation, F.J., I.M., J.M., L.P., M.D. and R.Z-C.; Formal analysis, J.M., L.P. and
549 M.D.; Investigation, F.J., I.M., J.M., L.P., M.D. and R.Z-C.; Resources, I.M. and R.Z-C.; Data
550 Curation, M.D.; Writing – original draft preparation, F.J., J.M., L.P. and M.D.; Writing – review and
551 editing, F.J., J.M. and M.D.; Visualization, M.D.; Supervision, F.J. and J.M.; Project administration,
552 F.J.; Funding acquisition, F.J., I.M., J.M., M.D. and R.Z-C.

553



554 **References**

- 555 Ali MH, Talukder MSU (2008) Increasing water productivity in crop production A synthesis. *Agr*
556 *Water Manage* 95:1201–1213. <https://doi.org/10.1016/j.agwat.2008.06.008>
- 557 Alkassem M, Buis S, Coulouma G, et al (2022) Estimating soil available water capacity within a
558 Mediterranean vineyard watershed using satellite imagery and crop model inversion. *Geoderma*
559 425:116081. <https://doi.org/10.1016/j.geoderma.2022.116081>
- 560 Ammar A, Riksen M, Ouessar M, Ritsema C (2016) Identification of suitable sites for rainwater
561 harvesting structures in arid and semi-arid regions: A review. *Int Soil Water Cons Res* 4:108–120.
562 <https://doi.org/10.1016/j.iswcr.2016.03.001>
- 563 Anderson W, Johansen C, Siddique KHM (2016) Addressing the yield gap in rainfed crops: a review.
564 *Agron Sustain Dev* 36:18. <https://doi.org/10.1007/s13593-015-0341-y>
- 565 Araya A, Kisekka I, Gowda PH, Prasad PVV (2017) Evaluation of water-limited cropping systems in
566 a semi-arid climate using DSSAT-CSM. *Ag Syst* 150:86–98.
567 <https://doi.org/10.1016/j.agsy.2016.10.007>
- 568 Besbes M, Chahed J, Hamdane A (2014) Sécurité hydrique de la Tunisie: gérer l'eau en conditions de
569 pénuries. l'Harmattan, Paris
- 570 Blinda M, Thivet G (2009) Ressources et demandes en eau en Méditerranée : situation et perspectives.
571 *Sécheresse* 20:009–016. <https://doi.org/10.1684/sec.2009.0162>
- 572 Bracken LJ, Croke J (2007) The concept of hydrological connectivity and its contribution to
573 understanding runoff-dominated geomorphic systems. *Hydrol Process* 21:1749–1763.
574 <https://doi.org/10.1002/hyp.6313>
- 575 Chen L, Sela S, Svoray T, Assouline S (2016) Scale dependence of Hortonian rainfall-runoff
576 processes in a semiarid environment: scale dependence of semiarid rainfall-runoff processes. *Water*
577 *Resour Res* 52:5149–5166. <https://doi.org/10.1002/2015WR018315>
- 578 Coulouma G, Ciampalini R, Annabi M, et al (2017) Synthèse de la prospection pédologique sur le
579 bassin versant de kamech dans le cadre du projet MASCC. UMR LISAH, Montpellier
- 580 Cousin I, Buis S, Lagacherie P, et al (2022) Available water capacity from a multidisciplinary and
581 multiscale viewpoint. A review. *Agron Sustain Dev* 42:46. [https://doi.org/10.1007/s13593-022-](https://doi.org/10.1007/s13593-022-00774-8)
582 00774-8

583 Daccache A, Elbana MA, Fouial A, et al (2016) Gestion des ressources en eau. In: *Mediterra: zéro*
584 *gaspillage en Méditerranée : ressources naturelles, alimentations et connaissances*. Centre
585 international de hautes études agronomiques méditerranéennes (CIHEAM) et Organisation des
586 Nations unies pour l'alimentation et l'agriculture (FAO).

587 Daryanto S, Wang L, Jacinthe P-A (2017) Global synthesis of drought effects on cereal, legume, tuber
588 and root crops production: A review. *Agr Water Manage* 179:18–33.
589 <https://doi.org/10.1016/j.agwat.2016.04.022>

590 Dhouib M, Zitouna-Chebbi R, Prévot L, et al (2022) Multicriteria evaluation of the AquaCrop crop
591 model in a hilly rainfed Mediterranean agrosystem. *Agr Water Manage* 273:107912.
592 <https://doi.org/10.1016/j.agwat.2022.107912>

593 Fader M, Giupponi C, Burak S, et al (2020) A 2020 Water. In: *Climate and Environmental Change in*
594 *the Mediterranean Basin – Current Situation and Risks for the Future*. First Mediterranean
595 Assessment Report. Union for the Mediterranean, Plan Bleu, UNEP/MAP Marseille France, pp. 181-
596 236

597 García-López J., Lorite I.J., García-Ruiz R. et al. (2014) Evaluation of three simulation approaches for
598 assessing yield of rainfed sunflower in a Mediterranean environment for climate change impact
599 modelling. *Climatic Change* **124**, 147–162. <https://doi.org/10.1007/s10584-014-1067-6>

600 Gnouma R (200-) Aide à la calibration d'un modèle hydrologique distribué au moyen d'une analyse
601 des processus hydrologiques : application au bassin versant de l'Yzeron PhD dissertation, INSA
602 Lyon.

603 Hamblin AP, Tennant D (1987) Root length density and water uptake in cereals and grain legumes:
604 how well are they correlated. *Aust J Agric Res* 38:513–527. <https://doi.org/10.1071/ar9870513>

605 Hossain A, Sab AE, Barutcular C, et al (2020) Sustainable crop production to ensuring food security
606 under climate change: A Mediterranean perspective. *Aust J Crop Sci* 14:439–446.
607 <https://doi.org/10.3316/informit.121077065862236>

608 Howes DA, Abrahams AD (2003) Modeling runoff and runon in a desert shrubland ecosystem,
609 Jornada Basin, New Mexico. *Geomorphology* 53:45–73. <https://doi.org/10.1016/S0169->
610 [555X\(02\)00347-1](https://doi.org/10.1016/S0169-555X(02)00347-1)

611 Jones OD, Sheridan GJ, Lane PN (2013) Using queuing theory to describe steady-state runoff-runon
612 phenomena and connectivity under spatially variable conditions. *Water Resour Res* 49:7487–7497.
613 <https://doi.org/10.1002/2013WR013803>

614 Jourdan R (2022) L'agriculture pluviale face aux changements climatiques en Afrique du Nord –

- 615 Impact et perspective avec l'agroécologie. FAO. Tunis. <https://doi.org/10.4060/cc0014fr>
- 616 Karabulut AA, Crenna E, Sala S, Udias A (2018) A proposal for integration of the ecosystem-water-
617 food-land-energy (EWFLE) nexus concept into life cycle assessment: A synthesis matrix system for
618 food security. *J Clean Prod* 172:3874–3889. <https://doi.org/10.1016/j.jclepro.2017.05.092>
- 619 Lange MA, Llasat MC, Snoussi M, et al (2020) First Mediterranean Assessment Report – Chapter 1:
620 Introduction. In: *Climate and Environmental Change in the Mediterranean Basin – Current Situation*
621 *and Risks for the Future. First Mediterranean Assessment Report, Union for the Mediterranean, Plan*
622 *Bleu, UNEP/MAP, Marseille, France, pp. 41-58. doi:10.5281/zenodo.7100592.*
- 623 Liu J, Lobb DA (2021) An Overview of Crop and Crop Residue Management Impacts on Crop Water
624 Use and Runoff in the Canadian Prairies. *Water-Sui* 13:2929. <https://doi.org/10.3390/w13202929>
- 625 Liu K, Harrison MT, Shabala S, et al (2020) The State of the Art in Modeling Waterlogging Impacts
626 on Plants: What Do We Know and What Do We Need to Know. *Earth's Future* 8:.
627 <https://doi.org/10.1029/2020EF001801>
- 628 Mbava N, Mutema M, Zengeni R, et al (2020) Factors affecting crop water use efficiency: A
629 worldwide meta-analysis. *Agr Water Manage* 228:105878.
630 <https://doi.org/10.1016/j.agwat.2019.105878>
- 631 Mekki I, Albergel J, Ben Mechlia N, Voltz M (2006) Assessment of overland flow variation and blue
632 water production in a farmed semi-arid water harvesting catchment. *Phys Chem Earth Parts A/B/C*
633 31:1048–1061. <https://doi.org/10.1016/j.pce.2006.07.003>
- 634 Mekki I, Zitouna-Chebbi R, Jacob F, et al (2018) Impact of land use on soil water content in a hilly
635 rainfed agrosystem: a case study in the Cap Bon peninsula in Tunisia. *AGROFOR* 3:.
636 <https://doi.org/10.7251/AGRENG1801064M>
- 637 Molénat J, Barkaoui K, Benyoussef S, et al (2023) Diversification from field to landscape to adapt
638 Mediterranean rainfed agriculture to water scarcity in climate change context. *Cur OpinEnv Sust*
639 65:101336. <https://doi.org/10.1016/j.cosust.2023.101336>
- 640 Molénat J, Raclot D, Zitouna R, et al (2018) OMERE: A Long-Term Observatory of Soil and Water
641 Resources, in Interaction with Agricultural and Land Management in Mediterranean Hilly
642 Catchments. *Vadose Zone J* 17:180086. <https://doi.org/10.2136/vzj2018.04.0086>
- 643 Nanda A, Sen S, McNamara JP (2019) How spatiotemporal variation of soil moisture can explain
644 hydrological connectivity of infiltration-excess dominated hillslope: Observations from lesser
645 Himalayan landscape. *J Hydrol* 579:124146. <https://doi.org/10.1016/j.jhydrol.2019.124146>



646 Nouri H, Stokvis B, Chavoshi Borujeni S, et al (2020) Reduce blue water scarcity and increase
647 nutritional and economic water productivity through changing the cropping pattern in a catchment. *J*
648 *Hydrol* 588:125086. <https://doi.org/10.1016/j.jhydrol.2020.125086>

649 Nunes AN, de Almeida AC, Coelho COA (2011) Impacts of land use and cover type on runoff and
650 soil erosion in a marginal area of Portugal. *Appl Geogr* 31:687–699.
651 <https://doi.org/10.1016/j.apgeog.2010.12.006>

652 Prosdocimi M, Jordán A, Tarolli P, et al (2016) The immediate effectiveness of barley straw mulch in
653 reducing soil erodibility and surface runoff generation in Mediterranean vineyards. *Sci Total Environ*
654 547:323–330. <https://doi.org/10.1016/j.scitotenv.2015.12.076>

655 Raes D, Steduto P, Hsiao TC, Fereres E (2009) AquaCrop -The FAO Crop Model to Simulate Yield
656 Response to Water: II. Main Algorithms and Software Description. *Agron J* 101:438–447.
657 <https://doi.org/10.2134/agronj2008.0140s>

658 Ramos MC, Martínez-Casasnovas JA (2006) Trends in Precipitation Concentration and Extremes in
659 the Mediterranean Penedès-Anoia Region, Ne Spain. *Climatic Change* 74:457–474.
660 <https://doi.org/10.1007/s10584-006-3458-9>

661 Saco PM, Rodríguez JF, Moreno-de las Heras M, et al (2020) Using hydrological connectivity to
662 detect transitions and degradation thresholds: Applications to dryland systems. *Catena* 186:104354.
663 <https://doi.org/10.1016/j.catena.2019.104354>

664 Schiettecatte W, Ouassar M, Gabriels D, et al (2005) Impact of water harvesting techniques on soil
665 and water conservation: a case study on a micro catchment in southeastern Tunisia. *J Arid Environ*
666 61:297–313. <https://doi.org/10.1016/j.jaridenv.2004.09.022>

667 Schoener G, Stone MC (2019) Impact of antecedent soil moisture on runoff from a semiarid
668 catchment. *J Hydrol* 569:627–636. <https://doi.org/10.1016/j.jhydrol.2018.12.025>

669 Souissi A, Mtimet N, Thabet C, et al (2019) Impact of food consumption on water footprint and food
670 security in Tunisia. *Food Sec* 11:989–1008. <https://doi.org/10.1007/s12571-019-00966-3>

671 Spinoni J, Vogt J, Naumann G, et al (2014) Towards identifying areas at climatological risk of
672 desertification using the Köppen-Geiger classification and FAO aridity index: towards identifying
673 areas at climatological risk of desertification. *Int J Climatol* 35:2210–2222.
674 <https://doi.org/10.1002/joc.4124>

675 Steduto P, Hsiao TC, Raes D, Fereres E (2009) AquaCrop-The FAO Crop Model to Simulate Yield
676 Response to Water: I. Concepts and Underlying Principles. *Agron J* 101:426–437.



677 <https://doi.org/10.2134/agronj2008.0139s>

678 Tadros MJ, Al-Mefleh NK, Othman YA, Al-Assaf A (2021) Water harvesting techniques for
679 improving soil water content, and morpho-physiology of pistachio trees under rainfed conditions. *Agr*
680 *Water Manage* 243:106464. <https://doi.org/10.1016/j.agwat.2020.106464>

681 Todorovic M, Albrizio R, Zivotic L, et al (2009) Assessment of AquaCrop, CropSyst, and WOFOST
682 Models in the Simulation of Sunflower Growth under Different Water Regimes. *Agron J* 101:509–
683 521. <https://doi.org/10.2134/agronj2008.0166s>

684 Toumi J, Er-Raki S, Ezzahar J, Khabba S., et al. (2016) Performance assessment of AquaCrop model
685 for estimating evapotranspiration, soil water content and grain yield of winter wheat in Tensift Al
686 Haouz (Morocco): Application to irrigation management, *Agric Water Manage* 163 :219-235.
687 <https://doi.org/10.1016/j.agwat.2015.09.007>

688 Van Gaelen H, Vanuytrecht E, Willems P, et al (2017) Bridging rigorous assessment of water
689 availability from field to catchment scale with a parsimonious agro-hydrological model. *Environ*
690 *Model Softw* 94:140–156. <https://doi.org/10.1016/j.envsoft.2017.02.014>

691 Van Leeuwen C (2022) 9 - Terroir: The effect of the physical environment on vine growth, grape
692 ripening, and wine sensory attributes. In: Reynolds AG (ed) *Managing Wine Quality* (Second
693 Edition). Woodhead Publishing, pp 341–393

694 Van Loo M, Verstraeten G (2021) A Spatially Explicit Crop Yield Model to Simulate Agricultural
695 Productivity for Past Societies under Changing Environmental Conditions. *Water-Sui* 13:2023.
696 <https://doi.org/10.3390/w13152023>

697 Wolka K, Mulder J, Biazin B (2018) Effects of soil and water conservation techniques on crop yield,
698 runoff and soil loss in Sub-Saharan Africa: A review. *Agr. Water Manage* 207:67–79.
699 <https://doi.org/10.1016/j.agwat.2018.05.016>

700 Yadari HE, Chikhaoui M, Naimi M, et al (2019) Techniques de conservation des eaux et des sols au
701 Maroc: Aperçu et perspectives. *Rev Mar Sci Agron Vet* 7 (2): 343-355

702 Yang H, Zehnder AJB (2002) Water Scarcity and Food Import: A Case Study for Southern
703 Mediterranean Countries. *World Dev* 30:1413–1430. [https://doi.org/10.1016/S0305-750X\(02\)00047-](https://doi.org/10.1016/S0305-750X(02)00047-5)
704 [5](https://doi.org/10.1016/S0305-750X(02)00047-5)

705 Zuecco G, Rinderer M, Penna D, et al (2019) Quantification of subsurface hydrologic connectivity in
706 four headwater catchments using graph theory. *Sci Total Environ* 646:1265–1280.
707 <https://doi.org/10.1016/j.scitotenv.2018.07.269>



708 **List of figures**

709

710 **Fig.1** :A typical Mediterranean hilly landscape showing hydrological connectivity (arrows) between
711 agricultural upstream and downstream plots (surrounded by a solid line) as well as the hydrographic
712 network (long dashed line). The landscape is located in Tunisia -Kamech catchment (© photo J.
713 Molénat).

714 **Fig. 2:** Representative diagram of the numerical experiment setting. It includes the spatial layout of
715 the two upstream (Up) and downstream (Do) plots, connected by runoff water from the upstream (R).
716 The table lists the factors considered for each plot, and the ranges of attributes/values are discussed
717 hereafter. Every crop ('crop X' or 'crop Y') corresponds to either to faba bean or wheat, the setup of
718 which is given in Section 2.3.1.

719 **Fig. 3:** Classification of climate years according to the FAO aridity index . Each year Y is a
720 hydrological year that spans from the beginning of September of calendar year [Y-1] to the end of
721 August of the year [Y].

722 **Fig. 4:** Occurrences of insignificant, positive, and negative relative differences calculated for wheat
723 (a) and for faba bean (b). The fully colored bars and the white bars outlined in color correspond to the
724 above ground biomass and the yield, respectively.

725 **Fig. 5:** Comparison of the temporal evolution of the (a) runoff (R) and precipitation (P), (b)
726 infiltration (Infl), (c) root zone water content (wRZ), (d) canopy cover (CC), (e) transpiration (Tr),
727 and (f) above ground biomass (AGB) among three different soil depths for wheat sown in 2002 in
728 clay-loam soil, with the same amount of infiltrated upstream runoff. CL-0.5 m, CL-1 m, and CL-1.5
729 m correspond to clay-loam soil depths of 0.5 m, 1 m, and 1.5 m, respectively. In all of these
730 simulations, the α ratio is 2, indicating that the upslope runoff (R) in (a), used as a water input, is
731 multiplied by 2.

732 **Fig. 6:** (a), (b) and (c) are monthly cumulative rainfall (Cum P), simulated runoff (Cum R) and
733 simulated infiltration (Cum Infi), respectively, in 2003 (blue bars) and 2004 (grey bars). (d) and (e)
734 are simulated water content in the root zone (wRZ) and simulated canopy cover (CC), respectively,
735 without connectivity in 2003 (blue line) and 2004 (grey line) for faba bean sown in a clay-loam soil
736 with a 1 m depth.

737

738 **List of tables**

739

740 **Table 1:** Crop parameters values used for AquaCrop simulations. Conservative (i.e., independent of
741 species, practices, and climate) and non-conservative (i.e., dependent on species, practices, and
742 climate) are presented (Alaya et al., 2019).

743

744 **Table 2:** Soil parameters values used for AquaCrop simulations. C, CL, and SCL correspond to clay,
745 clay-loam, and sandy-clay-loam textures, respectively. PWP, FC and Sat correspond to soil moisture
746 at the permanent wilting point, at field capacity and at saturation, respectively. Ksat corresponds to
747 saturated hydraulic conductivity.

748

749 **Table 3:** Classification of the cumulative values of upstream runoff. R1, R2, R3, and R4 correspond
750 to Classes 1, 2, 3, and 4, respectively, of cumulative values of upstream runoff. Q1, Q2, and Q3
751 correspond to the 1st quartile, median, and 3rd quartile, respectively.

752

753 **Table 4:** Percentage occurrence of significant and positive relative differences ($\Delta > 0.11$) categorized
754 by environmental factors. The abbreviations SH, DSH, and SA represent subhumid, dry subhumid,
755 and semiarid years, respectively. The labels R1, R2, R3, and R4 correspond to upstream runoff classes
756 1, 2, 3, and 4, respectively. The labels C, CL, and SCL stand for clay, clay-loam, and sandy-clay-loam
757 textures, respectively. AGB and Yld are the above ground biomass and the yield, respectively.

Table 1: Crop parameters values used for AquaCrop simulations. Conservative (i.e., independent of species, practices, and climate) and non-conservative (i.e., dependent on species, practices, and climate) are presented (Alaya et al., 2019).

CROP PARAMETERS	Wheat	Faba bean
Conservative parameters		
Base temperature (°C)	0	5.5
Cutoff temperature (°C)	26	30
Canopy cover per seedling at 90% emergence (CC ₀) (cm ²)	1.5	5
Canopy growth coefficient (CGC) (in fraction CC per GDD)	0.0052	0.0105
Maximum canopy cover (CC _x) in fraction soil cover	0.99	0.8
Crop coefficient for transpiration at CC = 100%	1.1	1.1
Decline in crop coefficient after reaching CC _x (%/day)	0.15	0.15
Canopy decline coefficient (CDC) (in fraction per GDD)	0.004	0.008
Water productivity normalised for ET ₀ and CO ₂ (WP*) (g/m ²)	13.4	13
Leaf growth threshold (Pupper)	0.2	0.25
Leaf growth threshold (Pflower)	0.65	0.6
Leaf growth stress coefficient curve shape	5	3
Stomatal conductance threshold (Pupper)	0.65	0.6
Stomata stress coefficient curve shape	2.5	3
Senescence stress coefficient (Pupper)	0.7	0.75
Senescence stress coefficient curve shape	2.5	3
Non conservative parameters		
GDD from sowing to emergence	140	122
GDD from sowing to maximum rooting depth	1670	741
GDD from sowing to start senescence	1861	1286
GDD from sowing to maturity (length of crop cycle)	2777	1411
GDD from sowing to flowering	1543	879
Length of the flowering stage (GDD)	189	128
GDD building up of harvest index during yield formation	980	495
Reference harvest index (HI ₀) (%)	45	30

Table 2: Soil parameters values used for AquaCrop simulations. C, CL, and SCL correspond to clay, clay-loam, and sandy-clay-loam textures, respectively. PWP, FC and Sat correspond to soil moisture at the permanent wilting point, at field capacity and at saturation, respectively. Ksat corresponds to saturated hydraulic conductivity.

SOIL PARAMETERS				
Hydrodynamic properties	Unit	Texture		
		C	CL	SCL
PWP	m ³ /m ³	0.39	0.23	0.20
FC	m ³ /m ³	0.54	0.39	0.32
Sat	m ³ /m ³	0.55	0.50	0.47
Ksat	mm/j	35	125	225

Table 3: Classification of the cumulative values of upstream runoff. R1, R2, R3, and R4 correspond to Classes 1, 2, 3, and 4, respectively, of cumulative values of upstream runoff. Q1, Q2, and Q3 correspond to the 1st quartile, median, and 3rd quartile, respectively.

Runoff class	Quartiles for the annual cumulative values of runoff
Class 1 (R1)	Cumulative annual runoff < 51 mm (Q1)
Class 2 (R2)	51 mm (Q1) ≤ Cumulative annual runoff < 95 mm (Q2)
Class 3 (R3)	95 mm (Q2) ≤ Cumulative annual runoff < 170 mm (Q3)
Class 4 (R4)	Cumulative annual runoff ≥ 170 mm (Q3)

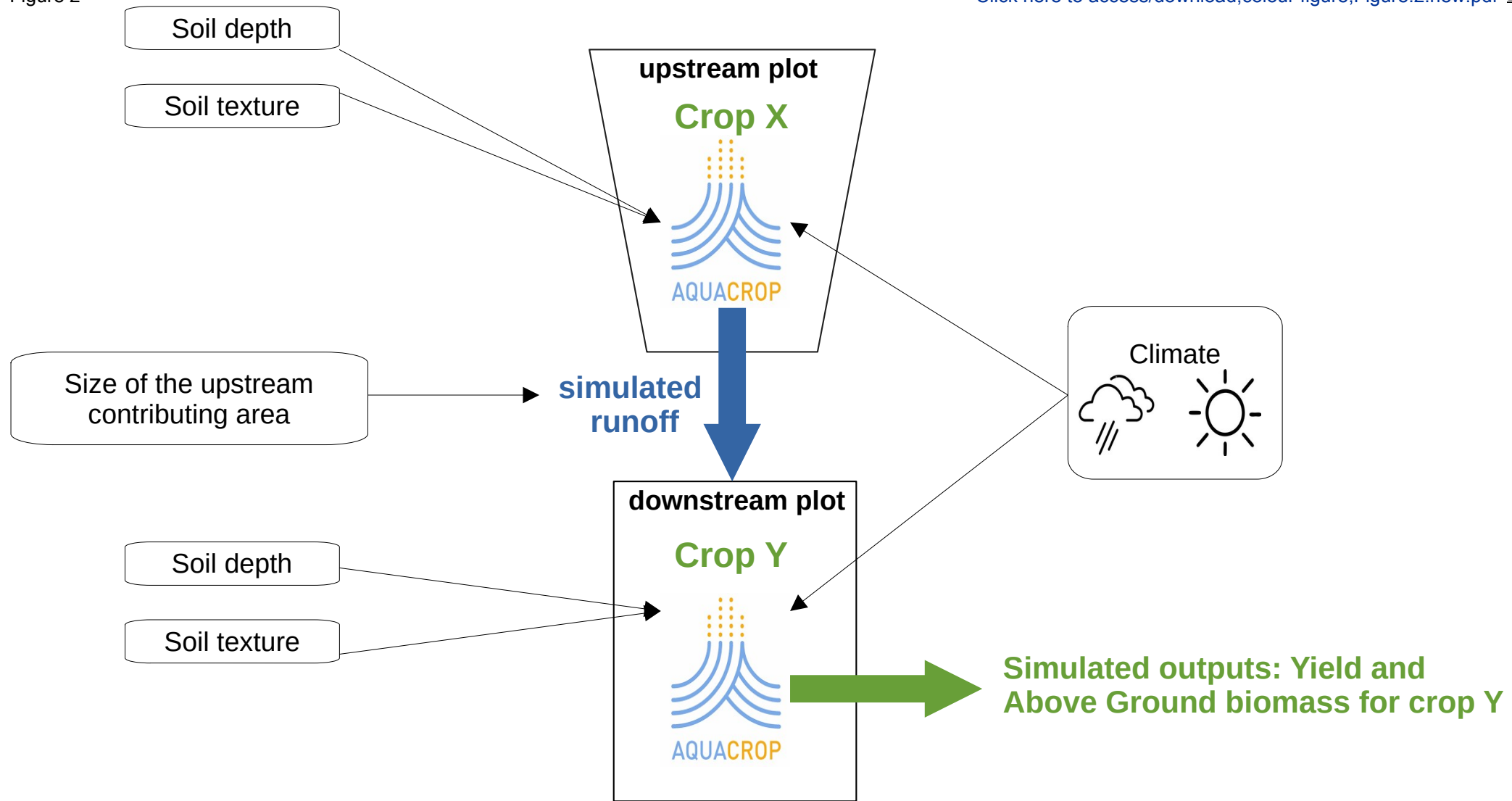
Table 4: Percentage occurrence of significant and positive relative differences ($\Delta > 0.11$) categorised by environmental factors. The abbreviations SH, DSH, and SA represent subhumid, dry subhumid, and semiarid years, respectively. The labels R1, R2, R3, and R4 correspond to upstream runoff classes 1, 2, 3, and 4, respectively. The labels C, CL, and SCL stand for clay, clay-loam, and sandy-clay-loam textures, respectively. AGB and Yld are the above ground biomass and the yield, respectively.

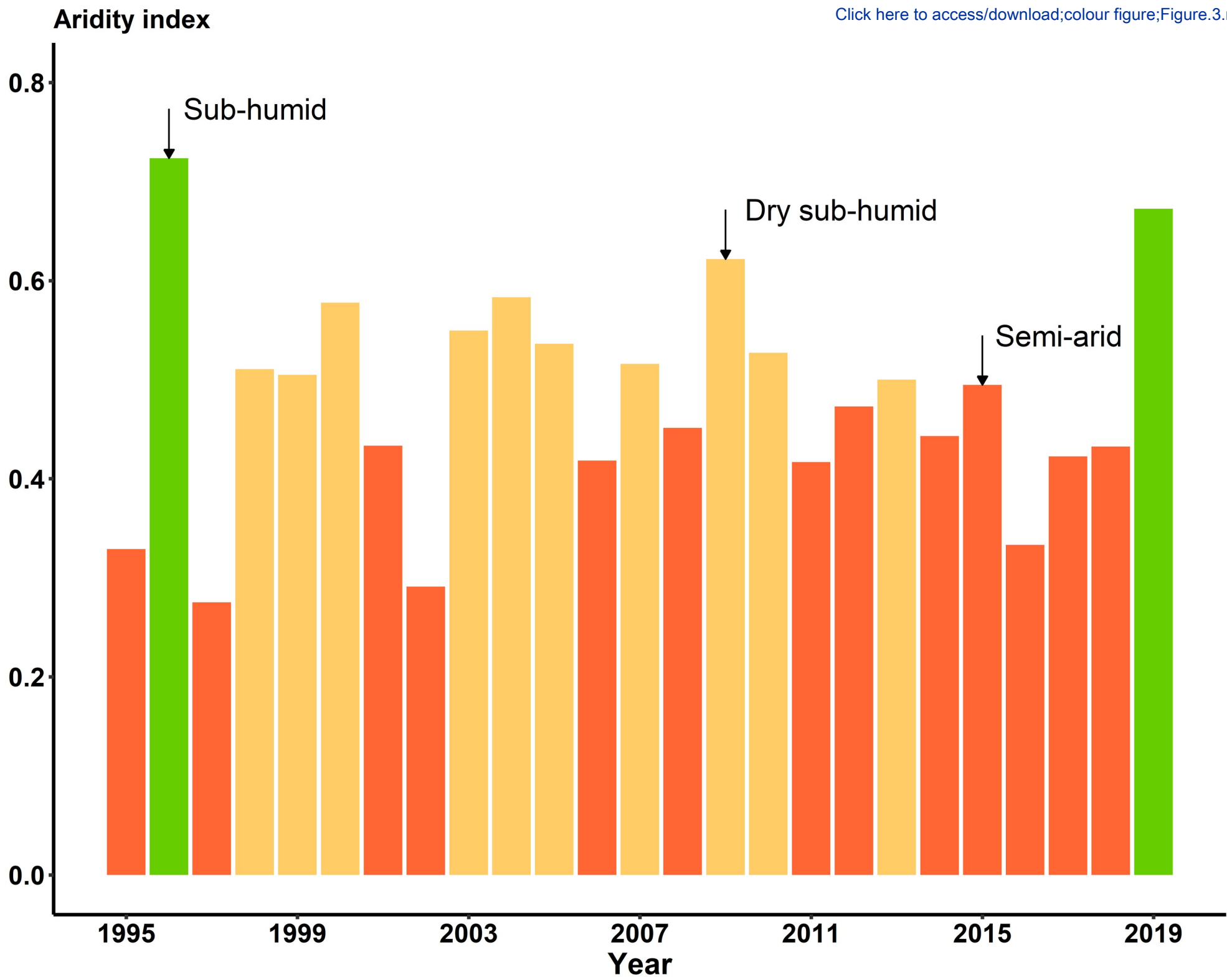
Crop	Variable	Climate			Upstream runoff				Texture			Soil depth		
		SH	DSH	SA	R1	R2	R3	R4	C	CL	SCL	0.5m	1.0m	1.5m
Wheat	AGB	0	44	56	22	24	27	27	33	45	22	12	31	57
	Yld	0	40	60	16	25	30	29	31	47	22	20	32	48
Faba bean	AGB	5	49	46	17	23	30	30	25	50	25	15	42	43
	Yld	4	45	51	18	24	28	30	29	45	26	15	42	43

Figure 1



Figure 2





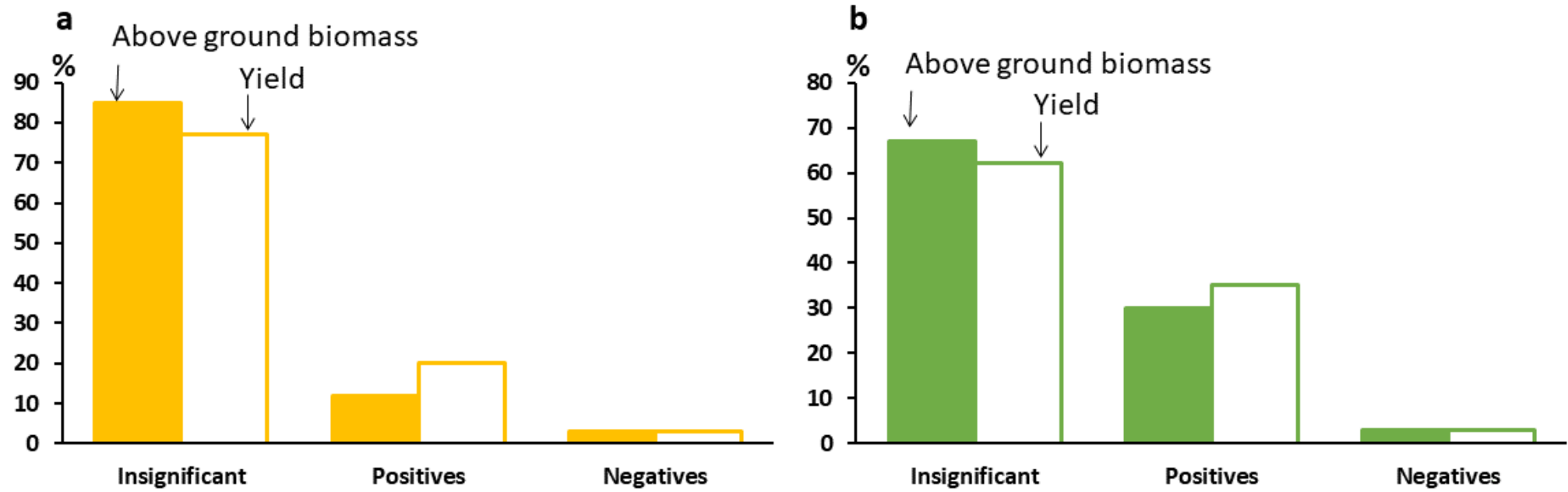


Figure 5

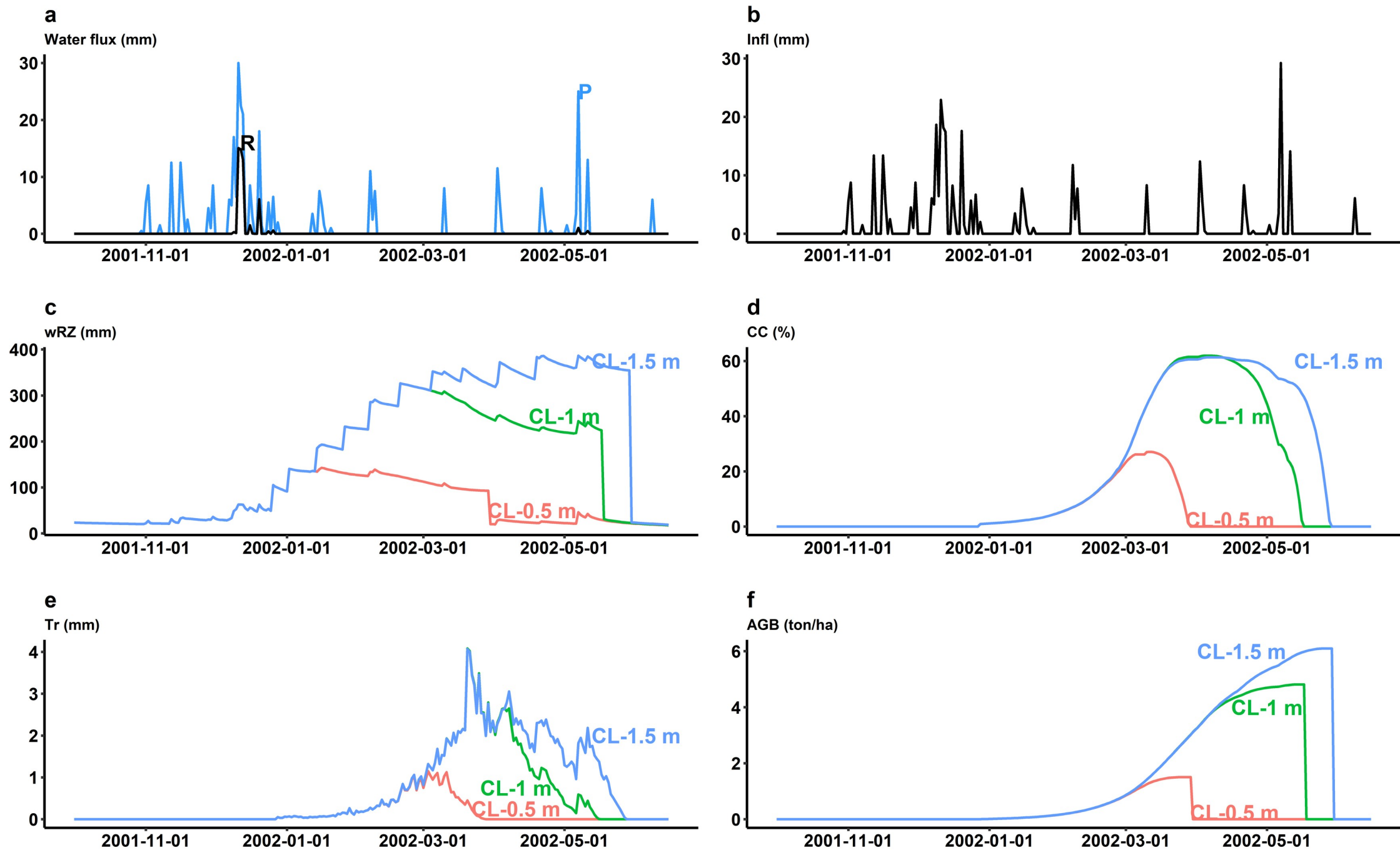
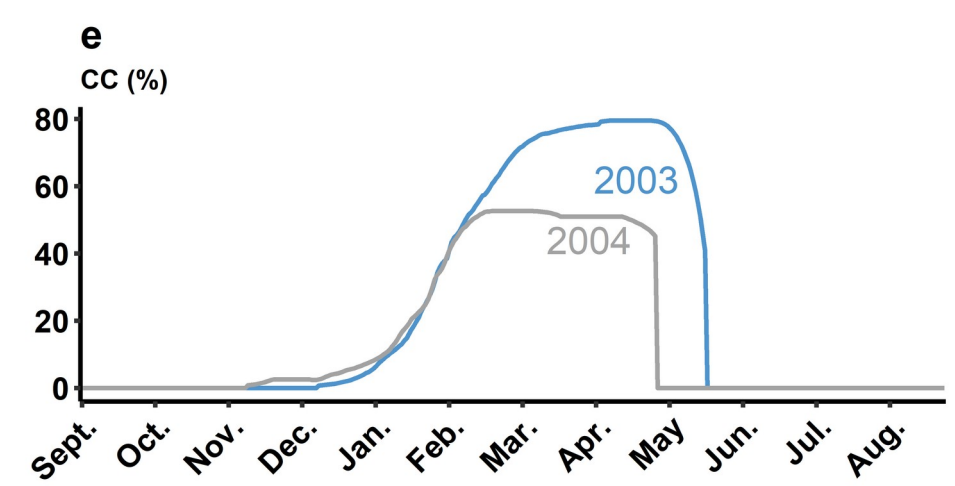
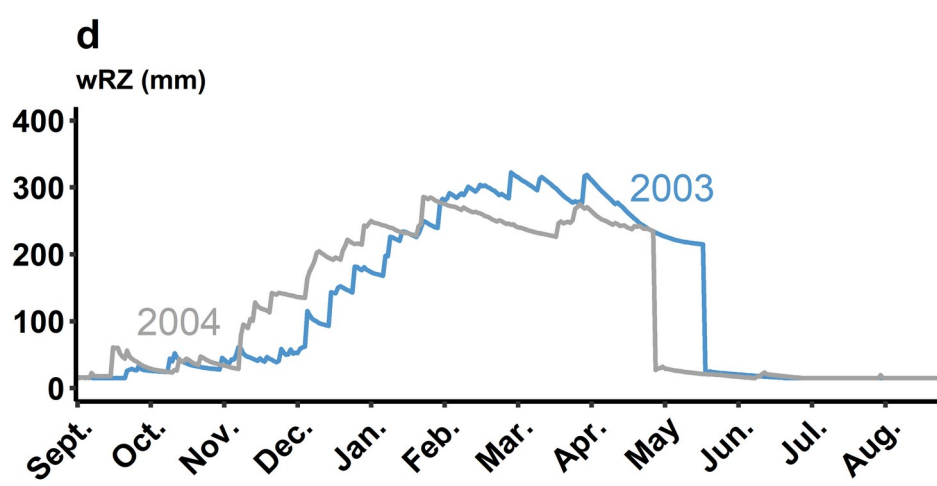
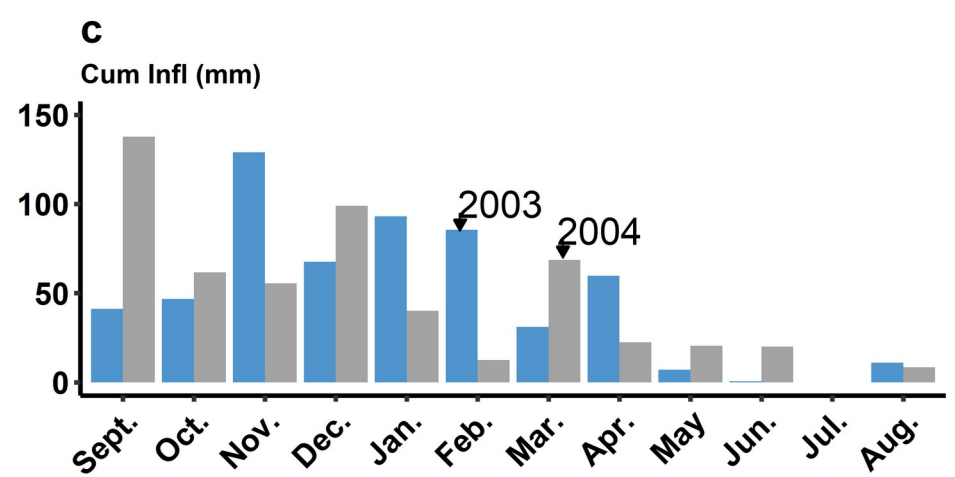
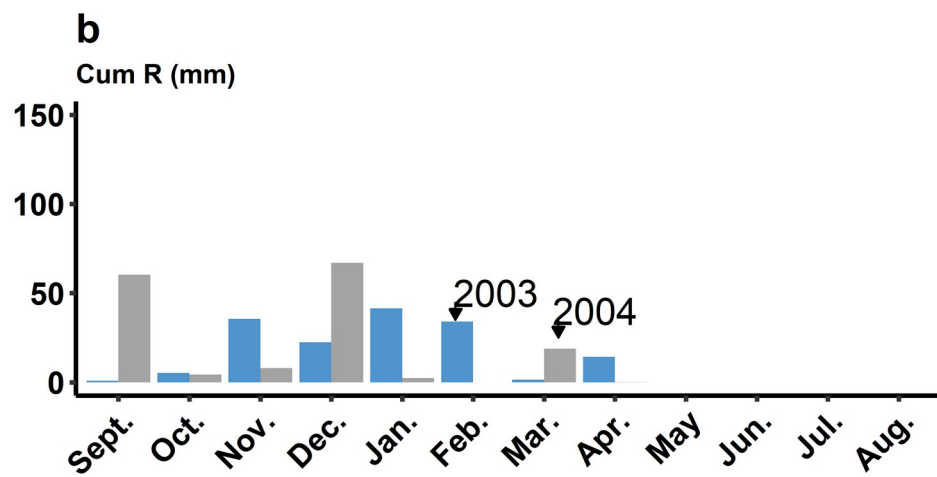
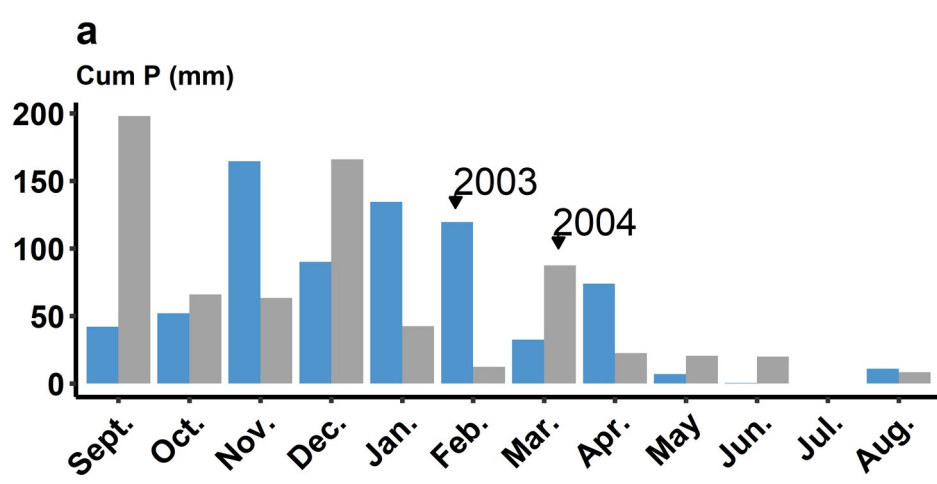


Figure 6



1
1
2
3
4
5
6
7
8
9
10
11
12
13
14
15

**Impact of hydrological connectivity on rainfed annual crops in Mediterranean hilly
landscapes: a numerical exploration**

**Mariam Dhouib¹, Jérôme Molénat¹, Laurent Prévot¹, Insaf Mekki², Rim Zitouna-Chebbi²,
Frédéric Jacob¹**

(1) LISAH, University of Montpellier, AgroParisTech, INRAE, Institut Agro, IRD, Montpellier,
France

(2) University of Carthage, National Research Institute of Rural Engineering, Water and Forests,
LR16INRGREF02-LRVENC, Rue Hédi Karray, 2080, Ariana, Tunisia

Supplementary materials

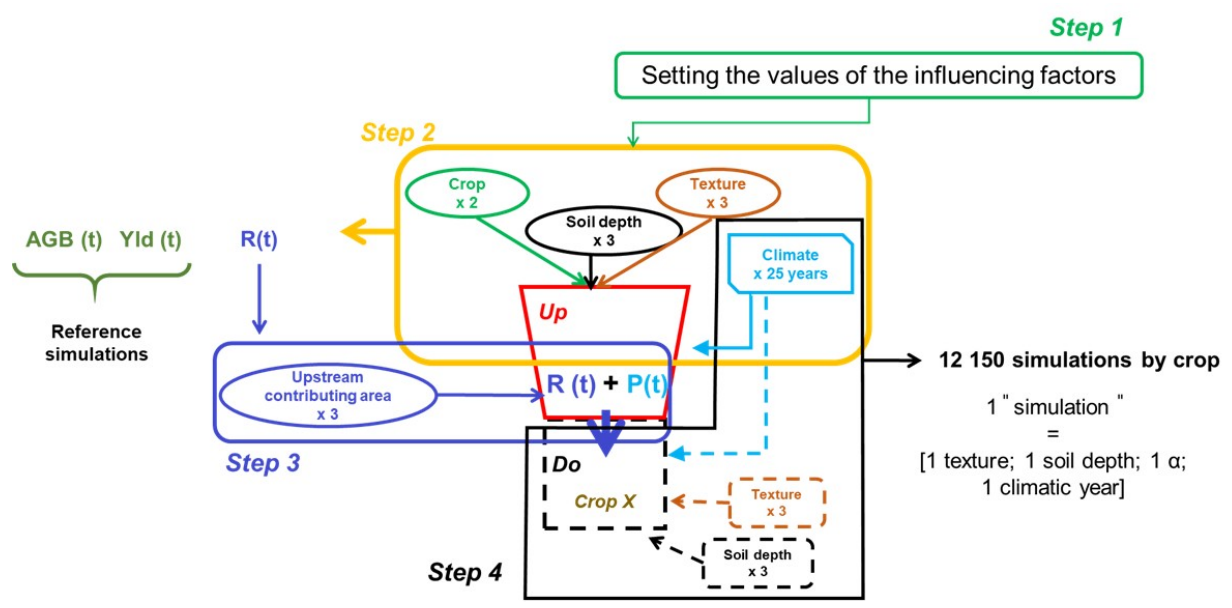
16 **Supplementary materials - Section 1: materials and methods - numerical experiment setting**

17 To assess the impact of hydrological connectivity on the functioning of the downstream crop, we
18 conduct a complete numerical experiment, including all possible combinations of the environmental
19 factors considered for both upstream and downstream plots, namely crops (wheat or faba bean), soil
20 water content availability (derived from soil texture and depth), and climate forcing variables that drive
21 water inputs (rainfall), water outputs (evaporative demand), and crop functioning (e.g., air temperature).
22 This also includes combinations with the upstream runoff. The simulation plan consists of four main
23 steps (Fig. SF 1) and results in 12 150 simulations for a given downstream crop on a yearly basis (Table
24 ST1), and therefore, in 24 250 simulations when considering the two downstream crops.

- 25 ● Step 1: Determination of the different values of the environmental factors, detailed in Sections 2, 3,
26 and 4 of the Supplementary Materials, except for soil parameters, which are listed in the current
27 section (Table ST1).
- 28 ● Step 2: AquaCrop simulations without connectivity. Once the different values of the environmental
29 factors are set, we conduct simulations on a single unconnected plot, considering all possible
30 combinations of textures (3), soil depths (3), and crops (2) over 25 years. At the end of this step, we
31 obtain, for each of the 18 combinations of texture/depth/crop, 25-year time series for runoff,
32 aboveground biomass, and yield. The time series of aboveground biomass and yield are considered
33 as reference time series (no connectivity) for assessing the impact of hydrological connectivity on
34 crop functioning.
- 35 ● Step 3: determination of upstream runoff time series. This step involves the runoff flux simulated in
36 Step 2, considered as a flux generated on the upstream plot that can infiltrate into the downstream
37 plot. This runoff flux is regarded as an incoming water flux at the upper limit of the downstream
38 plot. To account for the impluvium area, we consider three values for the upstream plot relative to
39 the area of the downstream parcel. For this, we set the ratio of upstream to downstream plot area,
40 labelled α , to three nominal values: 0.5, 1, and 2. Then, the values within each of the 18 simulated
41 runoff time series are multiplied by each of the three ratios α , resulting in 54 simulated runoff time
42 series that are added to rainfall on the downstream plot. At the end of this step, we obtain 54
43 upstream runoff time series over 25 years, and we add them to the rainfall time series over 25 years
44 for the downstream plot.
- 45 ● Step 4: AquaCrop simulations with connectivity. This step involves conducting AquaCrop
46 simulations for the downstream plot that receives the simulated runoff from the upstream plot
47 (Step 3). For each of the two downstream crops (wheat and faba bean) and each of the 9 situations in
48 terms of soil water available capacity (3 soil textures and 3 soil depths), we run 54 AquaCrop
49 simulations that include upstream runoff from Step 3. This results in $9 \times 54 = 486$ simulations of the
50 crop growth cycle, to be linked for further comparisons with the 9 AquaCrop simulations without
51 connectivity (reference time series at Step 2). On a yearly basis, the 486 simulations correspond to

5
52
53

486 x 25 = 12,150 simulations for each downstream crop, and thus 24,300 for both.



54
55
56
57
58

Fig. SF1: Overview of the 4 steps for the numerical experiment plan. AGB(t), Yld(t), R(t), and P(t) represent the time series of aboveground biomass, yield, upstream runoff, and rainfall, respectively, over 25 years. 'Up' and 'Do' labels stand for the upstream and downstream plots, respectively. The 'crop X' label for the downstream plot corresponds to faba bean or wheat.

59

60 **Table ST1:** Summary of different values for the considered environmental factors at each simulation step. C, CL, and SCL stand for Clay, Clay-Loam, and Sandy-Clay-Loam
 61 textures, respectively. Up and Do stand for upstream and downstream plots, respectively. R stands for upstream runoff. Cr, D, and T stand for crop, soil depth and texture,
 62 respectively. α stands for the ratio of the upstream to the downstream plot areas. AGB and Yld stand for aboveground biomass and grain yield. AC and SC stand for simulations
 63 with connectivity and without connectivity, respectively.

Simulation step	Field concerned	Crop (Cr)	Soil texture (T)	Soil depth (D, m)	Upstream plot area (α)	Combination number
Step 2	Field Up	{Wheat, Faba bean}	{C, CL, SCL}	{0.5, 1, 1.5}		2Cr x 3T x 3D = 18 SC simulations → 18 chronicles over 25 years for {R, AGB, Yld}
Step 3	Field Up				{0.5, 1, 2}	→ 18 chronicles of R x 3 α = 54 chronicles of R over 25 years
Step 4	Field Do	Wheat	{C, CL, SCL}	{0.5, 1, 1.5}	-	9 combinations {T, D} x 54 chronicles of R → 486 AC simulations over 25 years + 9 reference simulations without connectivity → 495 AC simulations over 25 years
		Faba bean	{C, CL, SCL}	{0.5, 1, 1.5}	-	9 combinations {T, D} x 54 chronicles of R → 486 AC simulations over 25 years + 9 reference simulations without connectivity → 495 AC simulations over 25 years

64

65

66 **Supplementary materials - Section 2: materials and methods - choice of sowing dates and** 67 **fertilisation rates for AquaCrop**

68 **Choice of sowing dates**

69 The sowing date is a crucial input parameter for running AquaCrop simulations. Setting this date for
70 each year and each crop is therefore an important step in the modelling process. An optimal sowing date
71 allows 1) to avoid germination failure due to lack of water at the beginning of the crop growth cycle and
72 2) to avoid the reduction of the growth time due to late sowing (Laux et al., 2010; Waongo et al., 2015).

73 We follow the sowing rules commonly set up within the study area for wheat and faba bean
74 cultivation (expert knowledge). For a given year, the sowing date is set by respecting the following
75 constraints.

- 76 ● The sowing period in the region: sowing must be carried out between October 20 and December 15
77 for wheat and between early November and late December for faba bean.
- 78 ● Cumulative rainfall since the beginning of the rainy season: the first date is chosen so that the
79 cumulative rainfall (calculated from September 1) is equal to or greater than 200 mm.
- 80 ● The daily rainfall amount on the chosen date: the sowing date is postponed by 5 days if the daily
81 cumulative rainfall on the chosen date is very high (exceeds 20 mm).

82 **Fertilisation rate**

83 For wheat fertilisation, we follow Dhouib et al. (2022) who set to 25% the value of fertilisation stress.

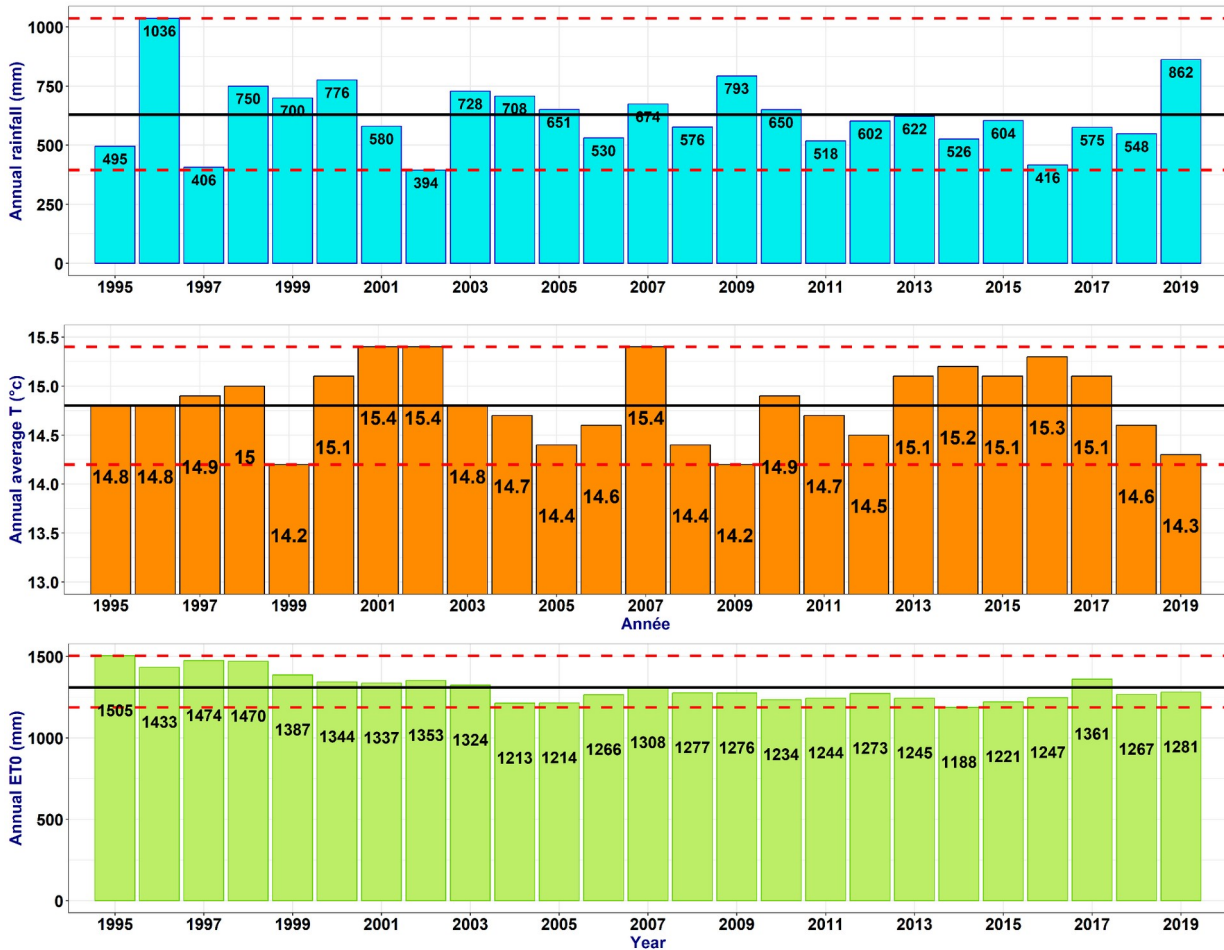
84 For faba bean, being a nitrogen-fixing legume, no fertilisation is necessary.

85

86 Supplementary materials - Section 3: materials and methods - climate forcing variables

87 Times series of climate variables

88



89

90 **Fig. SF2:** annual cumulative rainfall (1st row), annual average temperature (2nd row), and reference
 91 evapotranspiration (ET₀) (3rd row). Annual average temperatures (T) are calculated from October to May,
 92 corresponding to the growing season at the regional scale. The solid black line represents the average of each
 93 variable over the 25 years, and the dashed red lines represent the maximum and minimum cumulative values over
 94 the 25 years.

95 **Classification of climate conditions**

96 We characterise the annual climate using an aridity index, which serves as a proxy for soil water
97 availability according to soil-atmosphere exchanges (Nastos et al., 2013). We use the aridity index
98 proposed by FAO (FAO AI). This index expresses the degree of aridity as the ratio of the annual
99 cumulative rainfall P to the annual cumulative reference evapotranspiration ET_0 (Spinoni et al., 2015):

$$FAOAI = \frac{P}{ET_0} \quad (\text{SE 1})$$

100 The classification of climate years according to FAO AI is provided in Table ST3.

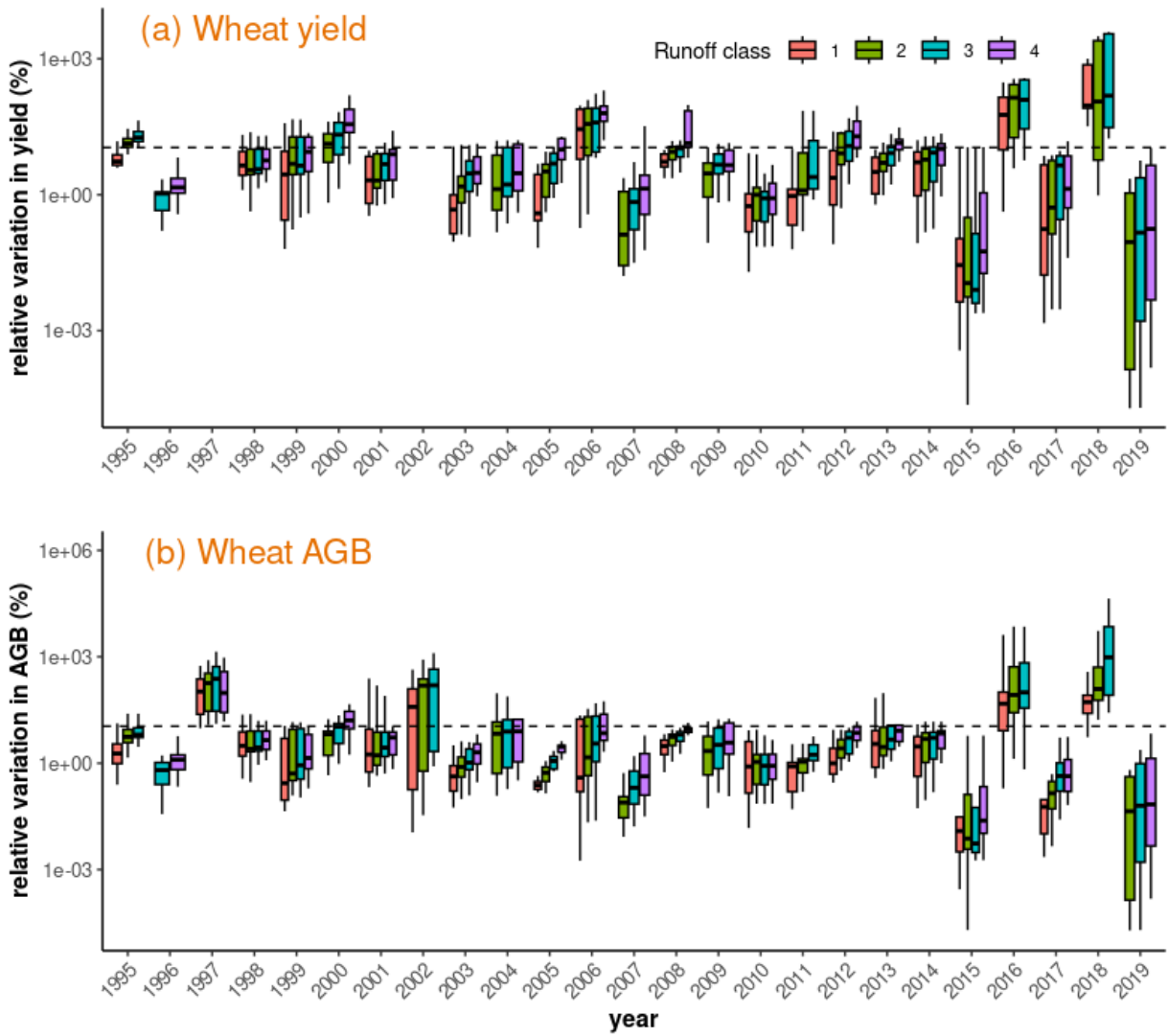
101

102 **Table ST2:** Aridity classification according to the FAO index.

FAO AI	Climate Class
[0.00 - 0.03[Desertic
[0.03 - 0.05[Hyper-arid
[0.05 - 0.20[Arid
[0.20 - 0.50[Semi-arid
[0.50 - 0.65[Dry sub-humid
[0.65 - 0.75[Sub-humid
[0.75 - 1.50[Humid
≥ 1.50	Hyper-Humid

103

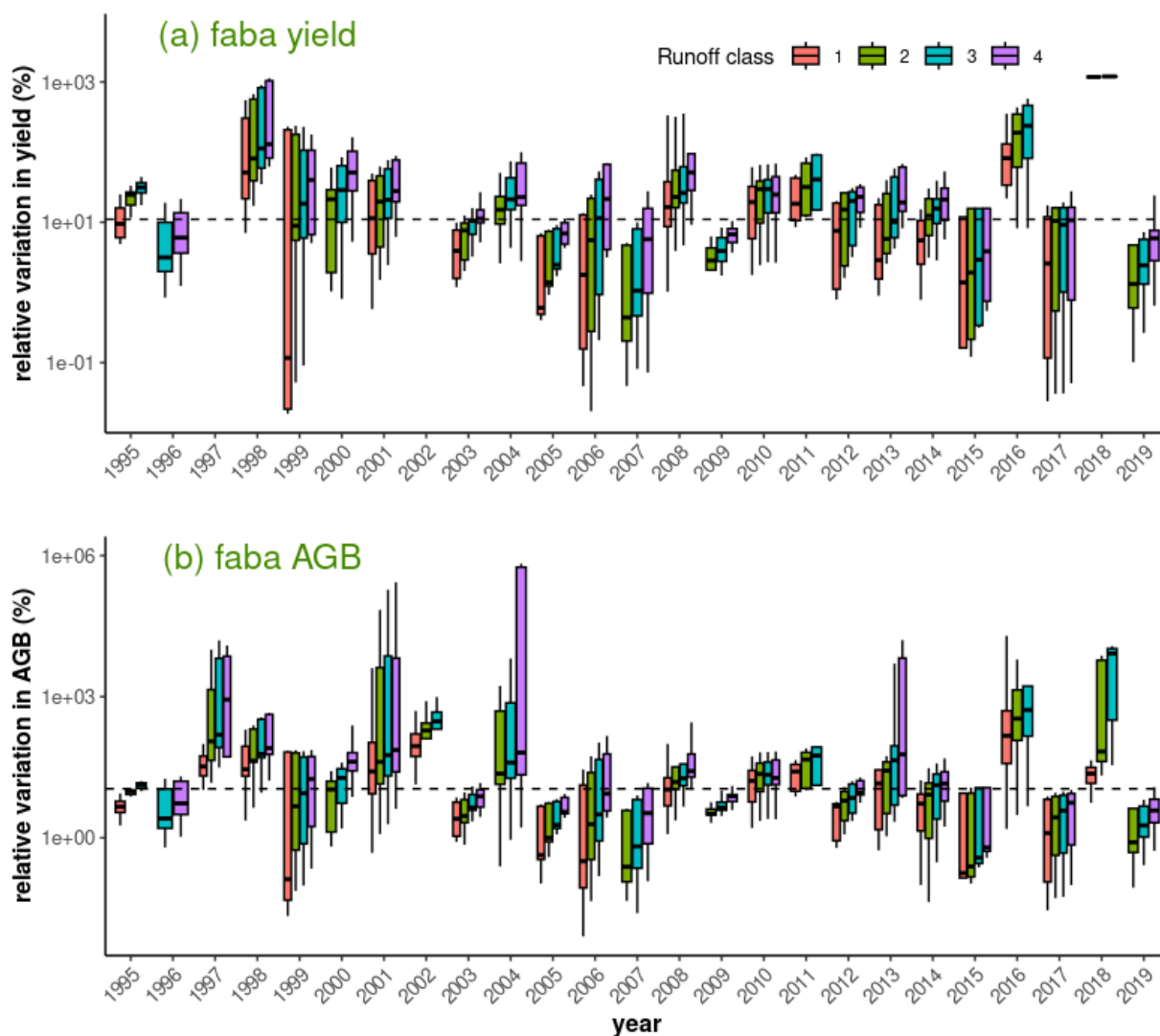
104



107 **Fig. SF3:** Relative variation (%) in yield (Yld) and Above Ground Biomass (AGB) over the 25-year
108 period for wheat crop considering each runoff class. The dashed line represents the level of significant
109 relative variation established in the study.

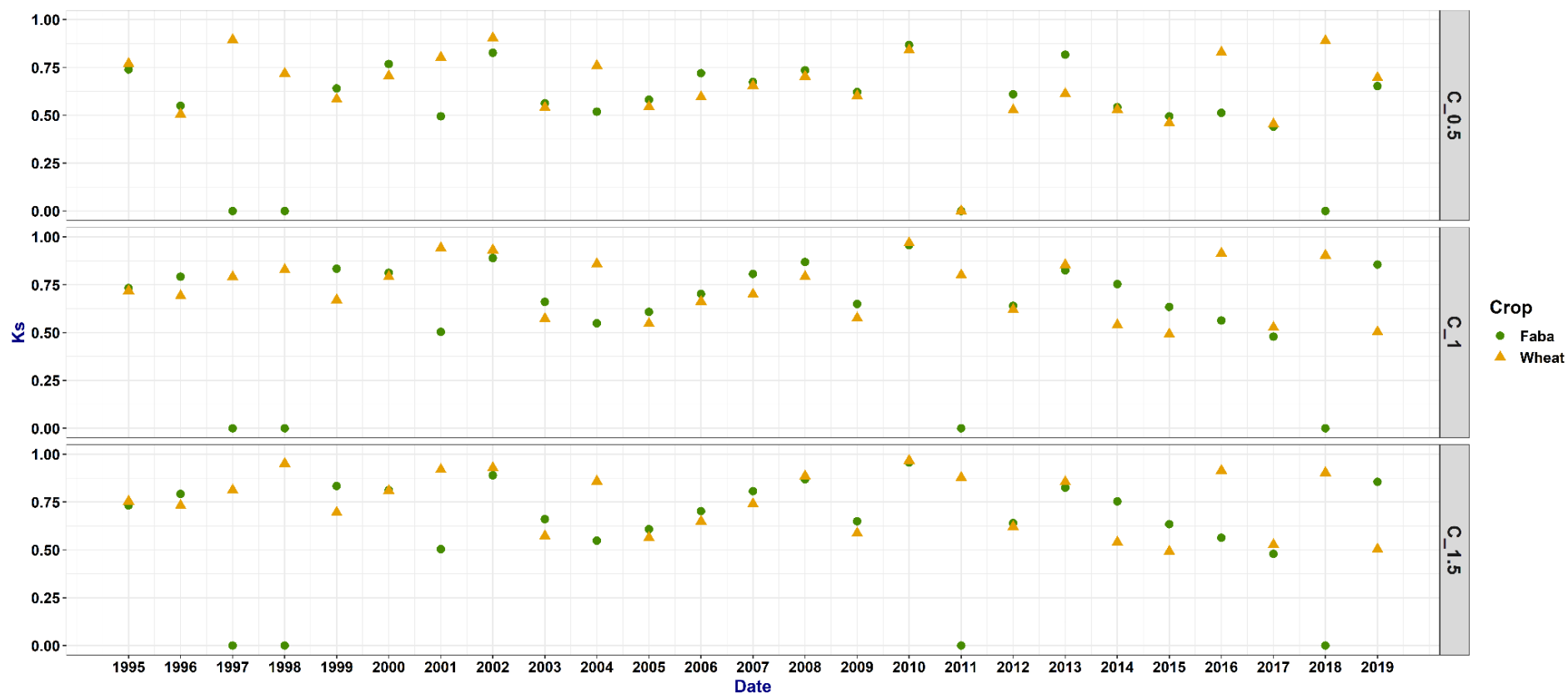
110

111



113 **Fig. SF4:** Relative variation (%) in yield (Yld) and Above Ground Biomass (AGB) over the 25-year
114 period for faba crop considering each runoff class. The dashed line represents the level of significant
115 relative variation established in the study.

116 **Supplementary materials - Section 5: results and discussion - water stress coefficient Ks**



117

118 **Fig. SF5 (part 1/3):** Mean water stress coefficient (Ks), calculated for faba bean (green disks) and wheat (yellow triangles) when considering simulations without connectivity.

119 A Ks equal to 1 corresponds to no water stress, while a Ks equal to 0 corresponds to full water stress. C represents Clay texture, respectively. The labels “_0.5”, “_1”, and

120 “_1.5” denote soil depths of 0.5 m, 1 m, and 1.5 m, respectively.

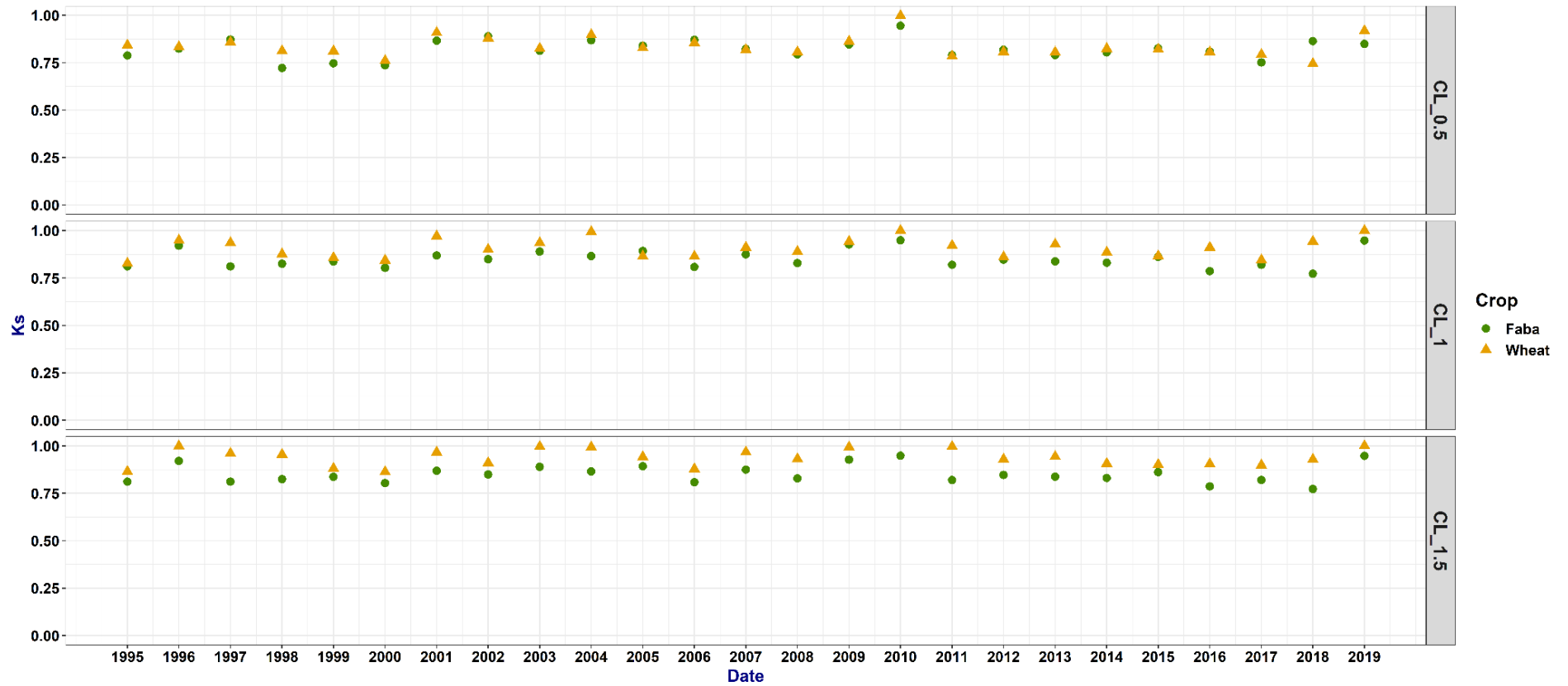
121

13

14

15

122

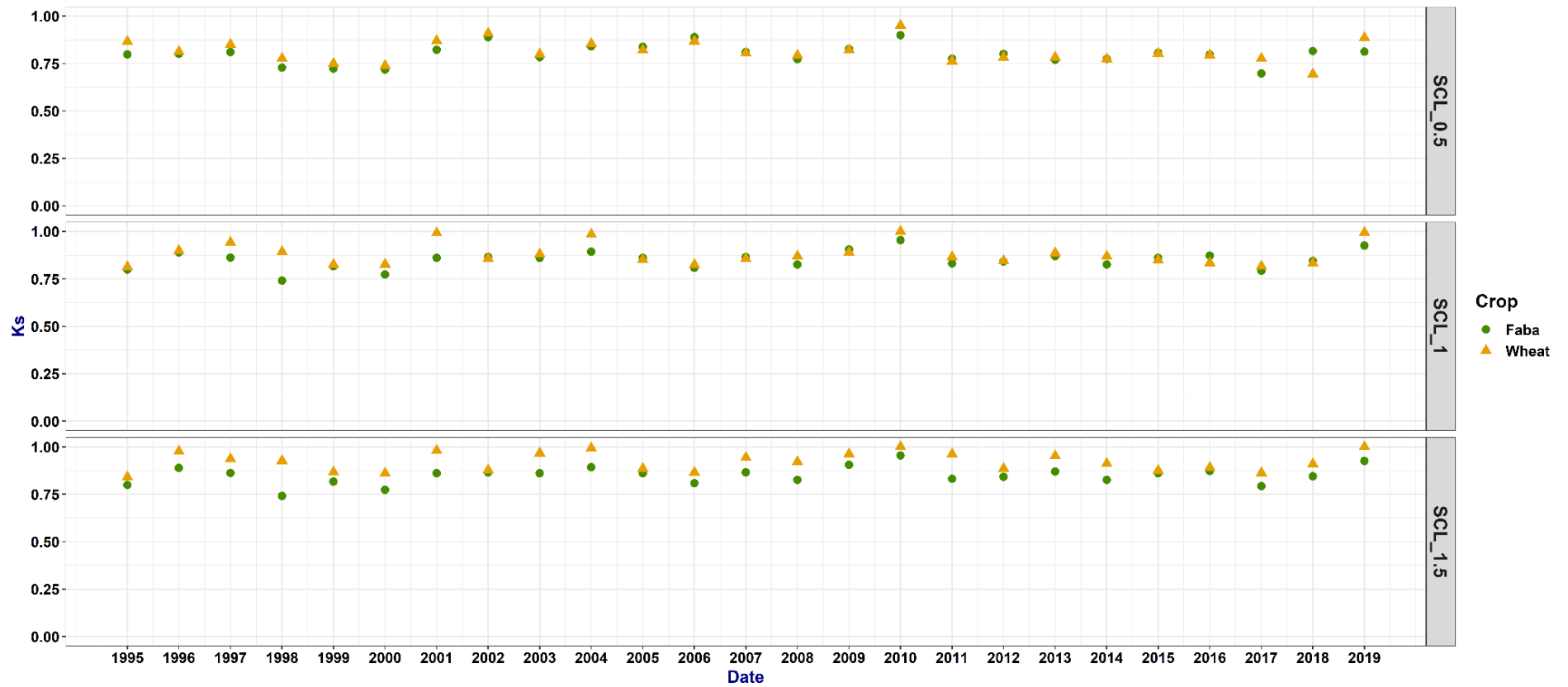


123

124 **Fig. SF5 (part 2/3):** Mean water stress coefficient (Ks), calculated for faba bean (green disks) and wheat (yellow triangles) when considering simulations without connectivity.
125 A Ks equal to 1 corresponds to no water stress, while a Ks equal to 0 corresponds to full water stress. CL represents Clay-Loam texture, respectively. The labels “_0.5”, “_1”,
126 and “_1.5” denote soil depths of 0.5 m, 1 m, and 1.5 m, respectively.

127

16
17
18



128

129 **Fig. SF5 (part 3/3):** Mean water stress coefficient (Ks), calculated for faba bean (green disks) and wheat (yellow triangles) when considering simulations without connectivity.
 130 A Ks equal to 1 corresponds to no water stress, while a Ks equal to 0 corresponds to full water stress. SCL represents Sandy-Clay-Loam texture. The labels “_0.5”, “_1”, and
 131 “_1.5” denote soil depths of 0.5 m, 1 m, and 1.5 m, respectively.

19
 20
 21

132 **Supplementary materials - Section 6: results and discussion - Influence of environmental**
 133 **condition**

134

135 **Table ST3:** Percentage occurrence of (1) insignificant relative differences ($-0.11 < \Delta < 0.11$) and (2) significant
 136 and positive relative differences ($\Delta > 0.11$) categorised by upstream runoff classes. The labels R1, R2, R3, and
 137 R4 correspond to upstream runoff classes 1, 2, 3, and 4, respectively.

Impact of hydrological connectivity	Crop	Variable	R1	R2	R3	R4
Insignificant impact	Wheat	AGB	26	25	25	24
		Yld	27	26	24	23
	Faba bean	AGB	29	26	23	22
		Yld	30	26	23	21
Positive impact	Wheat	AGB	22	24	27	27
		Yld	16	25	30	29
	Faba bean	AGB	17	23	30	30
		Yld	18	24	28	30

138

139 **Table ST4:** Average of relative difference calculated for infiltration (Infl), soil water content (SWC)
 140 and root zone water content (wRZ), for situations with positive impact and insignificant impact of hydrological
 141 connectivity. Relative differences correspond to differences between simulations with and without connectivity,
 142 and are next averaged over all situations (25 years, 54 upstream runoff, 9 downstream soil conditions). Infl is
 143 calculated over the hydrological year while SWC and wRZ are calculated over the crop growth cycle.

Impact	Crop	Relative differences (%)		
		Infl	SWC	wRZ
Positive impact	Wheat	10%	4%	41%
	Faba bean	7%	4%	24%
Insignificant impact	Wheat	8%	2%	2%
	Faba bean	6%	2%	1%

144

145

146 **Table ST5:** Average of relative difference calculated for infiltration (Infl), soil water content (SWC) and root
 147 zone content water (wRZ), for both situations with positive impact and insignificant impact of hydrological
 148 connectivity, in semi-arid (SA) and dry sub-humid (DSH) years. Relative differences correspond to differences
 149 between simulations with and without connectivity, and are next averaged over all situations (number of years
 150 for SA or DSH class, 54 upstream runoff, 9 downstream soil conditions). Infl is calculated over the hydrological
 151 year while SWC and wRZ are calculated over the crop cycle.

Climate year	Impact	Crop	Relative differences (%)		
			Infl	SWC	wRZ
SA	Positive impact	Wheat	9%	4%	29%
		Faba bean	7%	4%	18%
	Insignificant impact	Wheat	8%	2%	2%
		Faba bean	5%	2%	1%
DSH	Positive impact	Wheat	10%	4%	58%
		Faba bean	7%	4%	32%
	Insignificant impact	Wheat	9%	2%	2%
		Faba bean	6%	2%	1%

152

153

154

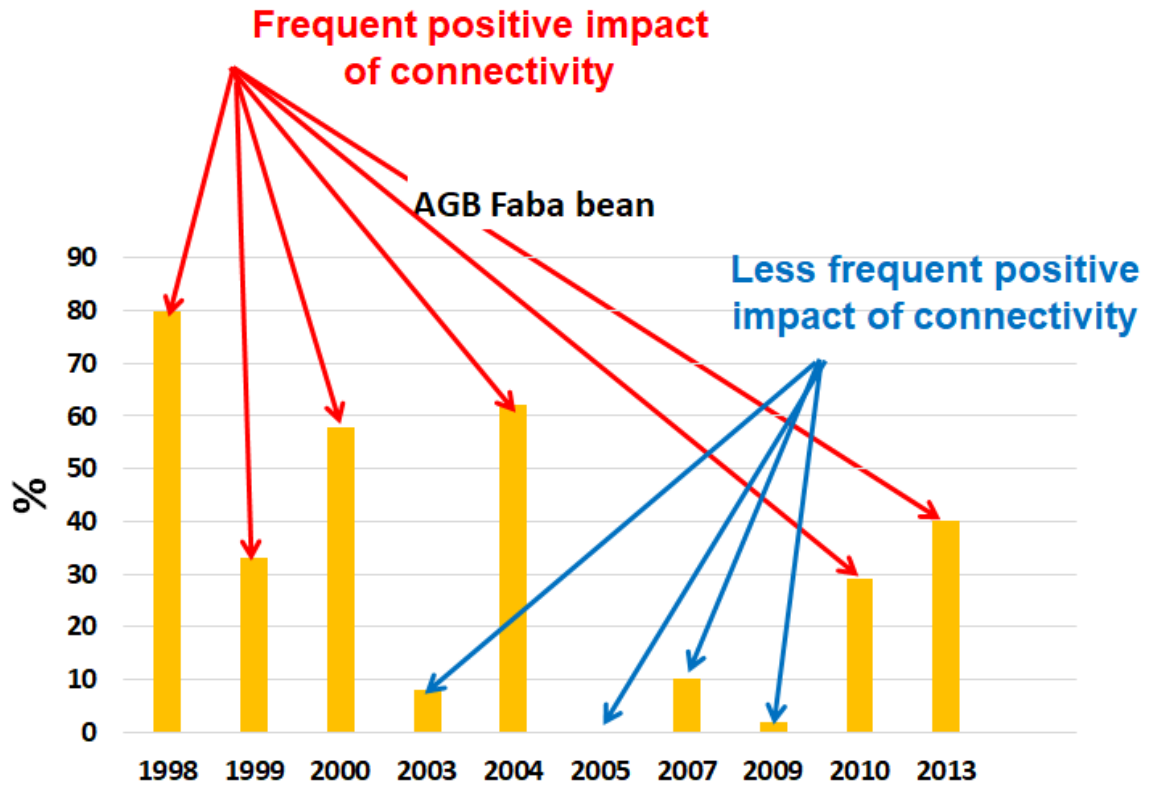
155

156

157

158

159



164 Fig. SF6: Occurrence in dry sub-humid years of positive impact ($\Delta > 0.11$) for faba bean.

166 **References**

- 167 Alaya, I., Masmoudi, M.M., Jacob, F., Ben Mechlia, N., 2019. Up-scaling of crop productivity
 168 estimations using the AquaCrop model and GIS-based operations. *Arabian Journal of*
 169 *Geosciences* 12. <https://doi.org/10.1007/s12517-019-4588-5>
- 170 Dhouib, M., Zitouna-Chebbi, R., Prévot, L., Molénat, J., Mekki, I., Jacob, F., 2022. Multicriteria
 171 evaluation of the AquaCrop crop model in a hilly rainfed Mediterranean agrosystem.
 172 *Agricultural Water Management* 273, 107912. <https://doi.org/10.1016/j.agwat.2022.107912>
- 173 Laux, P., Jäckel, G., Tingem, R.M., Kunstmann, H., 2010. Impact of climate change on agricultural
 174 productivity under rainfed conditions in Cameroon—A method to improve attainable crop
 175 yields by planting date adaptations. *Agricultural and Forest Meteorology* 150, 1258–1271.
 176 <https://doi.org/10.1016/j.agrformet.2010.05.008>
- 177 Nastos, P.T., Politi, N., Kapsomenakis, J., 2013. Spatial and temporal variability of the Aridity Index
 178 in Greece. *Atmospheric Research, advances in precipitation science* 119, 140–152.
 179 <https://doi.org/10.1016/j.atmosres.2011.06.017>
- 180 Spinoni, J., Vogt, J., Naumann, G., Carrao, H., Barbosa, P., 2015. Towards identifying areas at
 181 climatological risk of desertification using the Köppen-Geiger classification and FAO aridity
 182 index: towards identifying areas at climatological risk of desertification. *Int. J. Climatol* 35,
 183 2210–2222. <https://doi.org/10.1002/joc.4124>
- 184 Waongo, M., Laux, P., Kunstmann, H., 2015. Adaptation to climate change: The impacts of optimized
 185 planting dates on attainable maize yields under rainfed conditions in Burkina Faso.
 186 *Agricultural and Forest Meteorology* 205, 23–39.
 187 <https://doi.org/10.1016/j.agrformet.2015.02.006>

188